

REVIEW OF PHYSICS RESULTS FROM THE TEVATRON: HEAVY FLAVOR PHYSICS

JONATHAN LEWIS

*Fermi National Accelerator Laboratory
MS-318, P.O. Box 500
Batavia, IL 60510, United States
jdl@fnal.gov*

RICK VAN KOOTEN

*Department of Physics, Indiana University, Swain Hall West 117
Bloomington, IN 47405-7105, United States
rvankoot@indiana.edu*

We present a review of heavy flavor physics results from the CDF and DØ Collaborations operating at the Fermilab Tevatron Collider. A summary of results from Run 1 is included, but we concentrate on legacy results of charm and b physics from Run 2, including results up to Summer 2014.

Keywords: Tevatron, CDF, DØ, heavy flavor, charm, bottom, mesons, baryons, production, fragmentation, spectroscopy, decays, lifetimes, meson mixing, meson oscillations, CP violation, rare decays, flavor-changing neutral current decays.

PACS numbers: 12.38.Qk, 12.39.Hg, 12.39.Jh, 12.39.Ki, 12.39.Mk, 13.20.Fc, 13.20.Gd, 13.20.He, 13.25.Ft, 13.25.Gv, 13.25.Hw, 13.30.Ce, 13.30.Eg, 13.60.Le, 13.60.Rj, 13.87.Ce, 13.87.Fh, 14.20.Lq, 14.20.Mr, 14.40.Lb, 14.40.Nd, 14.40.Pq, 14.40.Rt, 14.65.Dw, 14.65.Fy,

Contents

1. Introduction and Context	3
2. Experimental Characteristics of Flavor Physics at the Tevatron	3
3. Historical Review: Run 1 Results	6
4. Production	8
4.1. Inclusive b and $b\bar{b}$	8
4.2. Charm	10
4.3. Quarkonia	10
4.4. Υ Polarization	12
4.5. b Fragmentation fractions	12
5. Spectroscopy	14
5.1. B mesons	14
5.2. Charm mesons	18
5.3. c and b -flavored baryons	18
5.4. Exotic States	20
6. Decays and Lifetimes	23
6.1. B meson lifetimes	23
6.2. b baryon lifetimes	24
6.3. Decay modes and branching ratios	26
7. Mixing and Oscillations of Heavy Neutral Mesons	27
7.1. Charm mixing	28
7.2. B^0 mixing and oscillations	29
7.3. B_s^0 mixing and oscillations	29
8. CP Violation	32
8.1. CP violation in charm	32
8.2. Direct CP violation in B decays	33
8.3. CP violation in B mixing	36
8.4. CP violation in interference between decay and B mixing	37
9. Rare Decays	39
9.1. FCNC decays of charm	40
9.2. FCNC decays of b hadrons	40
9.3. Lepton flavor violating decays	43
10. Summary	43

1. Introduction and Context

The flavor sector is that part of the standard model (SM) that arises from the interplay of quark weak gauge couplings and quark-Higgs couplings. The misalignment of these in the mass eigenstate basis gives rise to the Cabbibo-Kobayashi-Maskawa (CKM) matrix that encodes the physics of the weak flavor-changing decays of quarks. There are three generations of quarks and a very wide range of quark couplings and masses; however, we observe hadrons, not quarks. The top quark is so massive that it decays on timescales shorter than the typical hadronization time into other quarks. Bottom and charm quarks are therefore the most massive quarks that can comprise observable particles, and these are termed the “heavy flavor” hadrons. Their large mass often allows for relatively precise theoretical predictions via symmetries, perturbative QCD and the operator product expansion, heavy quark expansion, lattice QCD calculations, and QCD sum rules. Along the way, a great deal can be learned in the area of strong interactions that permits the probing of the weak physics of heavy flavors and the CKM matrix.

The production of heavy flavor hadrons tests QCD theory, and spectroscopy explores the interactions and dynamics of quarks inside of hadrons. Lifetimes and branching fractions straddle the boundary of weak decays and hadronic physics effects. The 3×3 CKM matrix allows for a CP -violating phase, and with enough independent measurements, it is possible to test SM predictions for CP violation. We know that the SM level of CP violation is not sufficient to explain the current matter-antimatter asymmetry of the universe, so we are continually searching for additional sources of CP violation due to physics beyond the standard model. The handy interferometric system of neutral heavy meson mixing and oscillations is another avenue to test CP violation as well as provide powerful constraints on CKM matrix elements. Finally, quantum effects in flavor loops can occur in any of the above areas and in cleanly predicted rare decays of heavy hadrons that in turn provide exquisitely sensitive probes for new physics. Following a description of the characteristics of heavy flavor physics at the Tevatron, all of the heavy flavor results from the CDF and DØ Collaborations in each of these areas are reviewed.

2. Experimental Characteristics of Flavor Physics at the Tevatron

The most appealing feature of hadron machines as tools to study b physics is their very high cross section for $b\bar{b}$ production. The Tevatron was a copious source of b hadrons with a production cross section four orders of magnitude greater than that at e^+e^- B factories. B factories operating at the $e^+e^- \rightarrow \Upsilon(4S)$ only produce B^0 and B^\pm mesons, and after LEP ceased operations, the Tevatron was a unique source for all the other heavier b hadrons such as B_s^0 , B_c^+ , b baryons, and all their excited states for more than a decade.^a

^aUnless otherwise stated, references to particles and processes include the charge conjugates as well.

Despite a very large production rate, b -quark events were a minuscule fraction of the overall $p\bar{p}$ event rate at the Tevatron. While the cross section for hadronic interactions at the Tevatron is about 50 mb, for the production of b and c quarks in the central region where the experiments have sensitivity, it is only about $10 \mu\text{b}$. Two features of heavy quarks make it possible to observe meaningful levels of signal among the enormous backgrounds. The first is the long lifetime of $\simeq 1.5 \text{ ps}$ for b hadrons, so that these boosted hadrons are likely to decay at secondary vertices a significant distance (of the order of a millimeter) from the beamline and interaction point of the $p\bar{p}$ beams. The reconstruction of these secondary vertices or the observation that a charged particle track is inconsistent with pointing back to the beamline is a powerful signature for identifying heavy flavor decays. Secondly, b hadrons have semileptonic branching ratios that are about 10% while it is rare for leptons to be produced in the prompt decays of light hadrons. Leptons are produced from interactions or decays at larger distances such as electrons from photon conversions, or muons from decays in flight of kaons and pions, but these backgrounds are small compared to inclusive hadron rates and can be studied and controlled. The situation for charm particles is more complicated. The lifetime and semileptonic branching ratio of D^+ mesons is similar to those for b hadrons; however, due to the large number of decay modes available to D^0 and D_s^+ mesons and to charm baryons, their lifetimes are considerably shorter and semileptonic branching ratios are smaller. Nonetheless, these signatures can be used for charm physics, albeit with more difficulty than in b -quark studies.

A cornerstone of b physics in hadron collider experiments is the signature provided by $B \rightarrow J/\psi X$ or $\psi' X$ with a branching fraction of approximately 1% followed by the decay of the ψ meson into $\mu^+\mu^-$ or e^+e^- . While the product branching fraction $B \rightarrow J/\psi \rightarrow \mu^+\mu^-$ is only $\simeq 6 \times 10^{-4}$, these decays provide a distinctive signature and are a rich source of information about the $b \rightarrow c\bar{c}s$ transition as well as providing triggering and tagging for the study of global properties of b hadrons.

Due to huge event rates, effective triggers and quality detectors are essential for extracting physics results. Heavy flavor analyses typically require detector strengths in three aspects of the experiments: triggering, reconstruction, and flavor tagging. Heavy quarks are produced in hadronic colliders preferentially at small polar angles θ (with respect to the beam axis) and at large absolute values of pseudorapidity $\eta \equiv -\ln[\tan(\theta/2)]$. Both experiments employed muons from $b \rightarrow \mu$ and $b \rightarrow c \rightarrow \mu$ for triggering. With a muon acceptance¹ in rapidity $|\eta| < 2$ that is twice as large as CDF's, the DØ detector has a distinct advantage in inclusive muon and dimuon triggering and studies. With less material before the first set of muon chambers, the CDF detector allows the study of dimuons with lower momenta. CDF's deadtimeless data acquisition system allowed for high-rate triggers based only on tracking information in the first level of the three-level system. Events so selected could be analyzed by the online silicon vertex tracker (SVT),² the first trigger processor developed to measure track impact parameters. The impact parameter resolution of the SVT was similar to that for offline reconstruction. The SVT gave CDF access

to a host of decay modes that include only charged hadrons in the final state. Electrons from semileptonic decays were included in the triggers of both experiments, but played a significantly lesser role in the physics program.

The upgraded CDF and DØ detectors^{3,4} also bring different strengths to reconstruction. With a much larger radius tracker, the CDF detector has superior momentum resolution leading to significantly better resolution on the reconstructed invariant masses of particles. This helps not only in the measurement of the masses themselves, but also with background rejection. The DØ detector gains from the larger rapidity acceptance of the tracker⁴ that extends out to $|\eta| < 3$. The impact parameter resolution of the CDF silicon detector⁵ and the DØ silicon microvertex tracker (SMT)⁶ (with a “Layer 0”⁷ added in 2006 partway through Run 2) are similar, approximately $30\ \mu\text{m}$ for tracks with typical momenta from b hadron decay with an asymptotic resolution of $10\text{--}15\ \mu\text{m}$ for high momentum single tracks. CDF also includes hadron identification with both specific ionization (dE/dx) measurement in the drift chamber³ and a time-of-flight (TOF) system⁸ comprising scintillator bars between the drift chamber and the solenoid. TOF measurements give unambiguous kaon identification for $p_T < 0.7\ \text{GeV}$, and at higher momenta the combination of dE/dx and TOF can be used on a statistical basis to separate particle types in reconstructed decays.

Flavor tagging in the context of heavy flavor physics is the determination of whether a particle with the potential of mixing or in a decay that is a CP eigenstate (e.g., $D^0 \rightarrow \pi^+\pi^-$) was created as a particle or anti-particle. In b physics, there are two types of flavor tags: away-side and same-side. In an away-side tag, the flavor of the other produced b hadron is used to determine the flavor of the one under study. These can be in the form of either a lepton presumably from a semileptonic decay or from the weighted sum of the charges of particles with displaced impact parameters. The rapidity of a b and \bar{b} are only weakly correlated, so the efficiency of making a tag is substantially better with DØ’s larger η range. However, these tags suffer from background and resolution effects that make the probability of an incorrect tag large as well. Same-side tags seek to identify the last particle created in the fragmentation process before the b hadron emerges. Thus a π^+ would be associated with a B^0 , a K^+ with a B_s^0 , and the negative tagging hadrons with a \bar{B}^0 or \bar{B}_s^0 meson. Same-side tags have high efficiency because they are associated with the B already within the detector acceptance. Given the large population of background pions, the TOF system in CDF was instrumental in employing the same-side kaon flavor tag in studies of B_s mixing. For charm physics, the key tag is the exploitation of the sign of the charge of the soft pion from $D^{*+} \rightarrow D^0\pi^+$ decays to determine the charm flavor.

For placing constraints on CP violation, the Tevatron also has an advantage of having a CP -invariant initial state of the $p\bar{p}$ beams and hence almost perfect CP -symmetric production in contrast to the LHC where production in pp collisions is not CP symmetric. In addition, the DØ detector has solenoidal and toroidal magnetic fields and consistently switched polarities of the magnets at regular two-week

intervals. As a result, differences in reconstruction efficiency between positively and negatively charged particles cancel to first order allowing high-precision measurements of charge asymmetries in the study of CP violation.

3. Historical Review: Run 1 Results

Early heavy flavor measurements at hadron colliders focused on production, which was a natural question given the new energy regime. Furthermore, it was widely believed that studies of bottom and charm particle decays would not be possible as a result of the many background particles present in hadron collisions. Access to heavy flavor events was limited as they could be found only in semileptonic decays that led to single high- p_T lepton triggers or in decays with quarkonium that produced dimuons which in turn provided the trigger signature.

The first high-energy collider was the $Spp\bar{S}$ at CERN which provided $p\bar{p}$ collisions at $\sqrt{s} = 546$ GeV where the UA1 collaboration pioneered the field using the spectra of transverse momentum p_T of leptons to deduce the spectrum of b -quark production.^{9–11} CDF made similar measurements in Run 0 (1987–89) at $\sqrt{s} = 1800$ GeV using inclusive electrons¹² and muons.¹³ After correcting for backgrounds, Monte Carlo simulations were used to derive an effective quark momentum threshold. Cross sections were not truly differential, but were quoted as the momentum $p_{T,b}$ such that 90% of leptons is a sample with some $p_{T,\ell}$ threshold resulted from quarks with momenta exceeding $p_{T,b}$. Because prompt production of J/ψ and ψ' mesons was thought to be minimal, these particles were also used to derive b hadron cross sections.¹⁴ The apparent discrepancies between the CDF and UA1 results and between the lepton and charmonium results were strong motivation for the production studies that would come in Run 1. In charm production, early measurements from both UA1¹⁵ and CDF¹⁶ were limited to the fraction of jets containing D^{*+} mesons.

CDF pioneered the full reconstruction of B mesons with a measurement¹⁷ of the B^+ meson cross section using the decay $B^+ \rightarrow J/\psi K^+$. The measurement¹⁸ of the average $B\bar{B}$ mixing fraction in dilepton events served as a determination of fraction of B_s^0 mesons in b -hadron production based on the $B^0\bar{B}^0$ mixing fraction observed in e^+e^- colliders at the $\Upsilon(4S)$ and the expectation of complete mixing for B_s^0 mesons.

Run 1 (1992–95) led to a revolution in thinking about heavy-quark physics at hadron colliders. While studies of heavy-quark production continued, CDF's installation of the SVX,¹⁹ the first silicon microvertex detector at a hadron collider, provided the opportunity not only to measure b hadron lifetimes^{20–29} but also a substantial reduction in backgrounds that was critical to measurements of b hadron masses.^{30,31} The riddle of large J/ψ and ψ' was at once solved and renewed with the measurement³² of differential production cross sections where the SVX could be used to separate prompt charmonium from that arising from b -hadron decays and showed the prompt fraction to be much larger than had been anticipated. Fur-

their work toward understanding quarkonium production included measurements of the Υ production spectrum,^{33–35} polarization in J/ψ , ψ' , and Υ decays,^{35,36} and the fractions of J/ψ and Υ that result from χ production.^{34,37,38} Measurements of b hadron cross sections were refined,^{39–41} and correlations⁴² between leptons and displaced tracks at both $\sqrt{s} = 1800$ and 630 GeV showed that theory properly described the energy scaling and that the apparent discrepancies between CDF and UA1 had to come from another source. The production fractions of b hadron species were also studied.^{43,44}

The low backgrounds afforded by the SVX also brought limits^{45–49} on rare decays and measurements^{50–57} of B meson decay properties such as the amplitudes in $B^+ \rightarrow J/\psi K^{(*)}$. A highlight of Run 1 is the discovery^{58,59} of the B_c meson with the measurement of its lifetime showing that the decay of the charm quark dominated the decay width. Based on the development of tagging techniques used in $B\bar{B}$ mixing measurements,^{60–64} CDF made and the first non-trivial limit on the CKM angle β from the measurement^{65,66} of $\sin 2\beta$ in $B^0 \rightarrow J/\psi K_S^0$ decays which set the stage for the mixing and CP -violation measurements that would come in Run 2.

The DØ detector did not participate in the first runs of the Tevatron (Run 0), but did join CDF in Run 1 operations beginning in 1992. The Run 1 DØ detector was optimized to meet the goals of excellent identification of electrons and muons, good measurement of parton jets at large p_T through a highly segmented calorimeter with very good energy resolution, and a well-controlled measure of missing transverse energy. The central design features⁶⁷ thus incorporated a compact, non-magnetic inner tracking volume with reasonable spatial resolution and particular emphasis on suppression of backgrounds to electrons. Via a toroidal magnetic field, the transverse momenta of muons could be determined, so invariant masses of only dimuon pairs could be found. The Run 1 DØ detector included a drift chamber vertex detector, so was able to reconstruct the impact parameters of tracks, but could not reconstruct invariant masses of long-lived heavy-flavor particles creating secondary vertices. b hadrons were identified via their semileptonic decays to muons, with the p_T of the muon relative to the jet axis used to separate charm semileptonic decays. As a result, the DØ heavy-flavor program in Run 1 was limited to b -quark and b -jet inclusive and differential cross section measurements,^{68–71} J/ψ cross section measurements,^{72,73} and a search for rare b decay.⁷⁴

To prepare for a vigorous heavy-flavor program for Run 2, the DØ detector upgrade⁴ maintained its excellent muon coverage and calorimetry, but now included a central magnetized tracker comprised of a superconducting solenoid surrounding a scintillating fiber tracker over a wide range of detector η plus a silicon microvertex tracker (SMT)^{6,7} which provided the benefits described above.

4. Production

4.1. Inclusive b and $b\bar{b}$

In hadron collisions, most production happens as $b\bar{b}$ pairs, either via s -channel production or gluon splitting, with a smaller fraction of b quarks produced by flavor excitation.⁷⁵ The total b production cross section is an interesting test of our understanding of QCD processes. As described in Section 3, past measurements of inclusive b quark production in the central rapidity region at Run 1 indicated a general agreement in shape with the calculated transverse momentum (p_T) spectrum, but were systematically higher than the NLO QCD predictions at the time by up to a factor of 2.5. With improved measurements, more accurate input parameters, and more advanced calculations, the discrepancy between theory and data is now much reduced.

Previous studies of b -quark production exploited the kinematic relationship between b quarks and daughter (semileptonic decay) muons and electrons to extract integrated b quark production rates. To avoid fragmentation and unfolding uncertainties, CDF chose to measure differential spectra for final-state bottom hadrons, while DØ references b jets rather than b quarks in Run 2, where b jets are defined as hadronic jets carrying b flavor. As opposed to quarks, jets or hadrons are directly observable and therefore reduce model dependence when comparing experimental data with theory and are in direct correspondence with a NLO QCD calculations. For instance, large logarithms that appear at all orders in the open quark calculation (due to hard collinear gluons) are avoided when all fragmentation modes are integrated.

The DØ Collaboration measured⁷¹ the inclusive b -jet cross section by tagging the jets using $b \rightarrow \mu$ semileptonic decay and the relatively high p_T of muons with respect to the jet axis to distinguish jets from charm and light flavor jets. As shown in Fig. 1, within experimental and theoretical uncertainties, DØ results are found to be higher than, but compatible with, next-to-leading-order QCD predictions. This result supersedes older Run 1 results^{68,69} for b -quark production (rather than jets).

CDF measured⁷⁶ the differential B^+ meson production spectrum using the decay mode $B^+ \rightarrow J/\psi K^+$ for $|y| < 1$. The total cross section was found to be $2.78 \pm 0.24 \mu\text{b}$ for $p_T > 6 \text{ GeV}$. Comparison to theory is more robust than in the case of the derived quark cross sections because the hard production and fragmentation can be calculated in a consistent framework. CDF also measured⁷⁷ the differential cross section of J/ψ mesons produced in b hadron decays. The fraction of J/ψ mesons from b hadron decays is determined by considering the displacement of the J/ψ decay points. Prompt mesons have a decay point consistent with the beamline, while those from the b decays will be displaced as a result of the long b lifetime. While event-by-event identification is not possible, the distributions are sufficiently distinct that prompt fractions can be measured in each momentum bin. Monte Carlo simulations are used to correct for the fraction of the parent b hadron momentum carried by the J/ψ mesons to yield a differential cross section for bottom hadrons

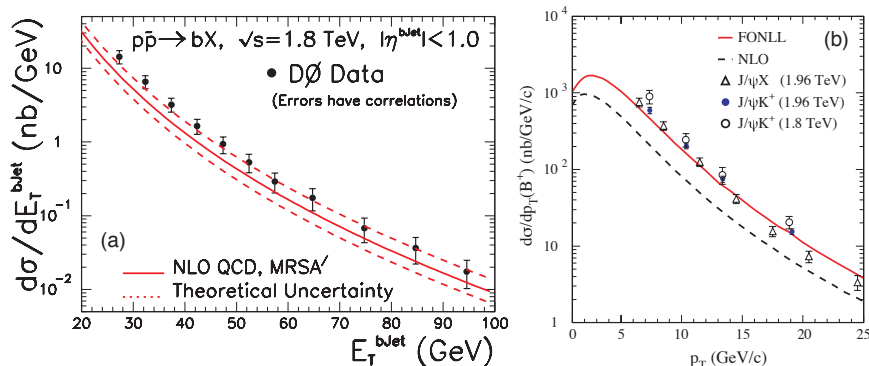


Fig. 1. (a) DØ measurement of the b -jet cross section; (b) CDF measurement of the B^+ cross section as well as the cross section of b hadrons inferred from displaced J/ψ mesons. For the later measurement and the theoretical predictions, the fragmentation fraction $f_u = 0.389$ is applied.

H_b . The results of both the B^+ and J/ψ measurements are shown in Fig. 1(b) along with results from Run 1.

CDF also measured the differential H_b cross section⁷⁸ using correlations of muons with D^0 or D^{*+} mesons. The $D^{(*)}\mu$ spectra are corrected in an analogous way to the displaced J/ψ spectra. The J/ψ , $\mu D^{(*)}$, and B^+ results are all in good agreement with each other and with the fixed-order leading log calculation of Refs. 79 and 80.

Measurements of both b quarks or b jets in the same event and their correlations have also been made at the Tevatron. Using samples of single muon and dimuon events from $b \rightarrow \mu$, the DØ Collaboration made an additional measurement of the b -quark cross section in a given kinematic range. As for previous b -quark measurements, the results agree in shape with the next-to-leading order QCD calculation of heavy flavor production but are greater than the central values of these predictions. The angular correlations between b and \bar{b} quarks, measured from the azimuthal opening angle between their decay muons, agree in shape with the next-to-leading order QCD prediction.

CDF used muon pairs to measure⁸¹ correlation in the production of b and \bar{b} quarks. The analysis considers the impact parameter distribution of muons with tight particle identification cuts to separate the component arising from $b\bar{b}$ from backgrounds including $c\bar{c}$ production and prompt-hadron fakes. For muons with $p_T \geq 3$ GeV that are produced by quarks with $p_T \geq 2$ GeV and $|y| < 1.3$, the measured cross section is $\sigma_{b \rightarrow \mu, \bar{b} \rightarrow \bar{\mu}} = 1549 \pm 133$ pb. This result is in general agreement with theoretical predictions and previous measurements.

The more precise cross section measurements of Run 2 demonstrated that the discrepancies between the Run 1 measurements and NLO predictions were significant and motivate the theoretical advances that can accurately model the production spectra.

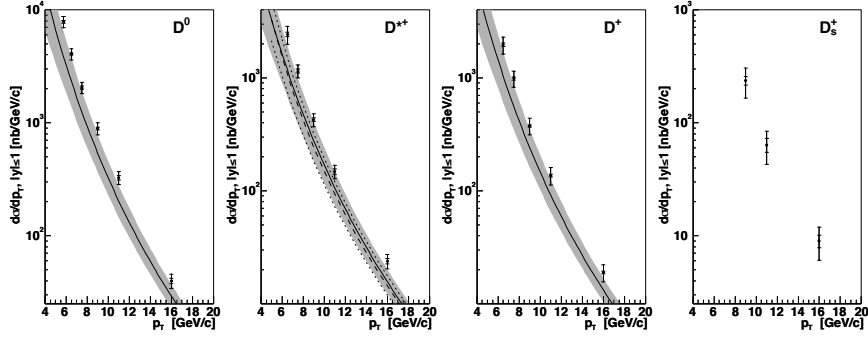


Fig. 2. CDF measurements of the differential cross sections of D^0 , D^{*+} , D^+ , and D_s^+ mesons

4.2. Charm

The differential charm meson cross section⁸² was one of CDF's first measurements in Run 2. The measurement is made using only 6 pb^{-1} of data collected with a displaced-track trigger. In the small dataset, the acceptance could be tightly controlled and therefore well modeled. There were no significant changes to the active channels in the detector over the course of the data used in the measurement. Even with the small dataset, the dominant uncertainties are systematic. As in the case of J/ψ cross section, secondary decays are accounted for on the basis of the impact parameter distribution. The differential cross sections are shown in Fig. 2 compared to the theory of Ref. 83.

4.3. Quarkonia

The study of heavy quarkonium production provides important information for perturbative and nonperturbative QCD, particularly factorization methods since heavy quark masses are larger than Λ_{QCD} , the typical scale where nonperturbative effects become significant. The nonperturbative evolution of the $Q\bar{Q}$ heavy-quark pair into a quarkonium has been discussed extensively in terms of models such as the color-singlet model (CSM), the color-evaporation model (CEM), the nonrelativistic QCD (NRQCD) factorization approach, and the fragmentation-function approach (see review of Ref. 84).

In high-energy $p\bar{p}$ collisions, J/ψ mesons can be produced in three ways: direct production, from the prompt decays of heavier charmonium states such as χ_{cJ} via $\chi_{cJ} \rightarrow J/\psi \gamma$, or from the decays of b hadrons, *i.e.*, $B \rightarrow J/\psi$.

A measurement⁸⁵ by the DØ Collaboration of double J/ψ production also included a measurement of the single J/ψ cross section. The decay length from the primary $p\bar{p}$ interaction vertex to the J/ψ production vertex determined via $J/\psi \rightarrow \mu^+ \mu^-$ was used to distinguish prompt from non-prompt J/ψ mesons to measure a cross section consistent with value calculated in the k_T -factorization

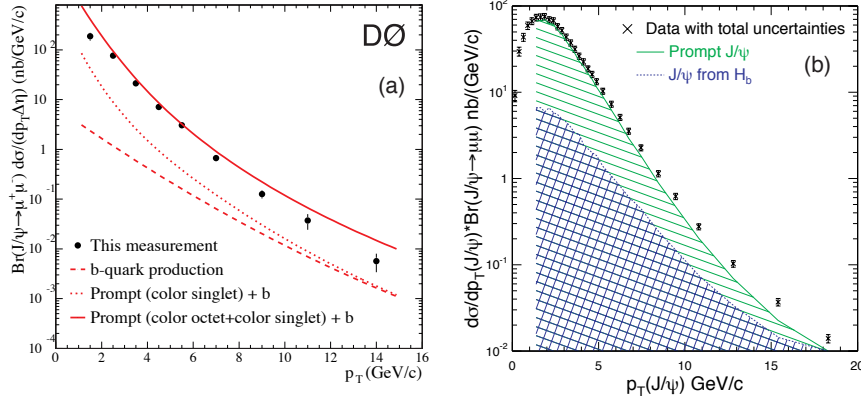


Fig. 3. (a) p_T dependence of the J/ψ differential cross section at $D\bar{D}$ and its theoretical predictions with only statistical uncertainties. The correlated uncertainty across all points is approximately 20%, including varying the J/ψ polarization between 0 and 100%. (b) CDF measurement of the inclusive J/ψ cross section as a function of J/ψ p_T integrated over the rapidity range $|y| < 0.6$.

approach⁸⁶ that includes direct production and that via χ_{cJ} . Two earlier measurements by the $D\bar{D}$ Collaboration using muon impact parameters to separate prompt from non-prompt production in the central region⁷² and at far forward angles⁷³ of $2.5 \leq |\eta^{J/\psi}| \leq 3.7$ showed rough agreement with the CEM in both p_T and η of the J/ψ and ruled out the CSM (see Fig. 3(a)). The former analysis measured a fraction of J/ψ mesons from χ_{cJ} decays to be significantly less than that predicted by direct charmonium production and gluon fragmentation.

CDF's measurement⁷⁷ of the inclusive J/ψ spectrum has been described above in Sect. 4.1 with results shown in Fig. 3(b). While the inclusive spectrum is measured down to zero transverse momentum, the prompt component can be separated only for $p_T > 1.25$ GeV. Because there are no $c\bar{c}$ states between the ψ' and the open-charm threshold, the ψ' cross section provides a clean test of production models compared to the J/ψ that is polluted by χ_c feed down. CDF measured the ψ' spectrum⁸⁷ using dimuon events. The method for separating prompt and secondary components is the same as in the J/ψ measurement. The results are consistent with gluon-tower models⁸⁸ which have large uncertainties. However, like the J/ψ cross section, ψ' production is poorly fit by NNLO QCD descriptions.⁸⁹

Bottomonium states are produced either promptly or indirectly as a result of the decay of a higher mass state, *e.g.*, in a radiative decay such as $\chi_b \rightarrow \Upsilon(1S)\gamma$, but with the advantage over charmonium of not being produced via the decays of other heavy flavor states leading to a simpler analysis as all states are prompt.

By reconstructing the $\Upsilon(1S)$ through its decay $\Upsilon(1S) \rightarrow \mu^+\mu^-$, the $D\bar{D}$ Collaboration has determined⁹⁰ production cross section of the $\Upsilon(1S)$ as a function of its transverse momentum, in three rapidity ranges. These are reasonably consis-

tent within theoretical and experimental uncertainties with theoretical models of the time,^{91,92} which are similar to the CEM, as are the ratios of the cross sections in different rapidity ranges. These results provide greater precision than the CDF Run 1 result.³⁵ CDF's other important result in the study of bottomonium from Run 1 is the fraction³⁴ of $\Upsilon(1S)$ mesons that are produced from χ_b decays which is found to be $(49.1 \pm 8.2 \text{ (stat)} \pm 9.0 \text{ (syst)})\%$ for $p_T > 8 \text{ GeV}$.

4.4. Υ Polarization

Theoretical models that were constructed to accommodate the surprisingly large production cross section of J/ψ and Υ mesons beyond the initial CSM also make specific predictions about their production polarization but were generally in poor agreement with initial experimental measurements. The angular distribution of muons from $\Upsilon \rightarrow \mu^+ \mu^-$ decays are described by the distribution:

$$\frac{d\Gamma}{d\Omega} \propto 1 + \lambda_\theta \cos^2 \theta + \lambda_\varphi \sin^2 \theta \cos 2\varphi + \lambda_{\theta\varphi} \sin 2\theta \cos \phi \quad (1)$$

in the Υ rest frame where the angles refer to the positive lepton with respect to the direction of the Υ . A convenient measure of the polarization is the variable $\alpha \equiv \lambda_\theta = (\sigma_T - 2\sigma_L)/(\sigma_T + 2\sigma_L)$ where σ_T and σ_L are the transversely and longitudinally polarized components of the production cross section, respectively.

The DØ Collaboration measured⁹³ the λ_θ polarization variable for the $\Upsilon(1S)$ meson using decays to $\mu^+ \mu^-$ as a function of $p_T(\Upsilon)$ as shown in Fig. 4(a), indicating strong longitudinal polarization for lower values of p_T . Discrepancies between results for λ_θ obtained by different experiments suggest that quarkonia might be strongly polarized when produced, but that different experimental acceptances can impact the final measurement. Early analyses measured only λ_θ as a function of $p_T(\Upsilon)$ in one reference frame; however, polarization could be manifested by significantly non-zero values of λ_φ or $\lambda_{\theta\varphi}$ even when λ_θ near zero.⁹⁴

While the observed lack of transverse polarization at high momentum in the helicity basis is inconsistent with NRQCD-inspired models, it is not a definitive demonstration of a lack of polarization in Υ production. To demonstrate that the production is truly unpolarized, CDF performed a full three-dimensional decomposition to measure⁹⁵ the three components of polarization λ_θ , λ_φ , and $\lambda_{\theta\varphi}$ in both the helicity and Collins-Soper frames for $p_T < 40 \text{ GeV}$ for $\Upsilon(1S)$, $\Upsilon(2S)$, and $\Upsilon(3S)$ decays to muon pairs. From the measured components, one can form the frame-invariant quantity $\tilde{\lambda} = (\lambda_\theta + 3\lambda_\varphi)/(1 - \lambda_\varphi)$. The results for $\tilde{\lambda}$ are shown in Fig. 4(b). The agreement between measurement in the two frames demonstrates a lack of systematic bias. The values near zero indicate that indeed the production of $\Upsilon(1S)$, $\Upsilon(2S)$, and $\Upsilon(3S)$ mesons is unpolarized.

4.5. b Fragmentation fractions

b quarks produced in $p\bar{p}$ collisions are accompanied by $q\bar{q}$ pairs created in the color field in the process of fragmentation where anti-quarks combine with the b quark to

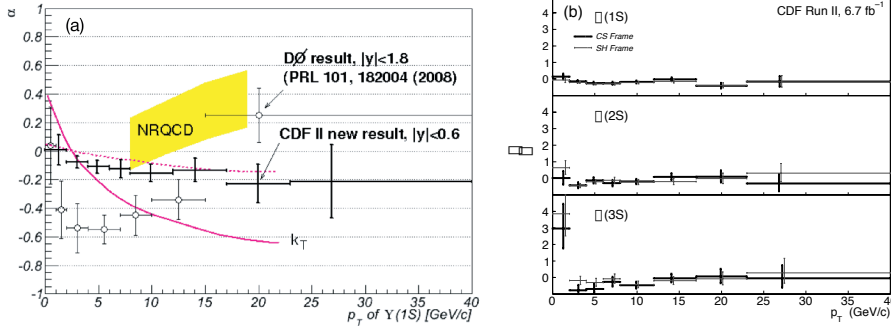


Fig. 4. (a) CDF and DØ results on Υ polarization compared to theoretical predictions for $\Upsilon(1S)$. The yellow bands indicates the range of $\alpha(\equiv \lambda_\theta)$ predicted by NRQCD.⁹⁶ The two magenta curves show two extreme cases of the k_T factorization model.⁹⁷ The upper (dashed) curve assumes complete de-polarization of the $\Upsilon(1S)$ when produced in the decay of χ_b states, while the lower (solid) curve assumes that the polarization is preserved. (b) CDF results on the frame-invariant quantity $\bar{\lambda}$ in the Collins-Soper frame and s -channel helicity frame.

form a B meson $|b\bar{q}\rangle$ or with di-quarks to form a b baryon $|bq_1q_2\rangle$. In contrast with the B factories operating at the $\Upsilon(4S)$ peak where only B^0 and B^\pm are produced, in high-energy collisions, all species of weakly decaying b hadrons may be produced, either directly or in strong and electromagnetic decays of excited b hadrons. The probabilities that the fragmentation of a b quark will result in a B^+ $|\bar{b}u\rangle$, B^0 $|\bar{b}d\rangle$, B_s^0 $|\bar{b}s\rangle$, or Λ_b $|bud\rangle$ are denoted as f_u , f_d , f_s , and f_{Λ_b} , respectively.

The DØ Collaboration has measured⁹⁸ the product $f_{\Lambda_b} \cdot \mathcal{B}(\Lambda_b^0 \rightarrow J/\psi \Lambda) = (6.01 \pm 0.88) \times 10^{-5}$.

CDF has measured⁹⁹ relative production fractions using the yields of ℓD^0 , ℓD^+ , ℓD^{*+} , ℓD_s^+ , and $\ell \Lambda_b^0$. After correcting for branching ratios updated¹⁰⁰ since the publication of the paper, the relative fractions are

$$\begin{aligned} \frac{f_u}{f_d} &= 1.054 \pm 0.018 \text{ (stat)}_{-0.045}^{+0.025} \text{ (syst)} \pm 0.058 \text{ (Br)}, \\ \frac{f_s}{f_u + f_d} &= 0.128 \pm 0.005_{-0.008}^{+0.009} \pm 0.011 \text{ (Br)}, \text{ and} \\ \frac{f_{\Lambda_b}}{f_u + f_d} &= 0.281 \pm 0.012 \text{ (stat)}_{-0.056}^{+0.058} \text{ (syst)}_{-0.086}^{+0.128} \text{ (Br)}. \end{aligned}$$

The first result is consistent with expectations from isospin, and the second agrees with results from LHCb.^{101,102} The baryon fraction is also in general agreement with LHCb; however, because it depends on momentum, a more detailed evaluation is required.

The Heavy Flavor Averaging group has used these as inputs to a global fit giving average and independent fragmentation fractions both for $p\bar{p}$ collisions at the Tevatron and for high energies (*i.e.*, LEP, Tevatron, LHC).¹⁰³

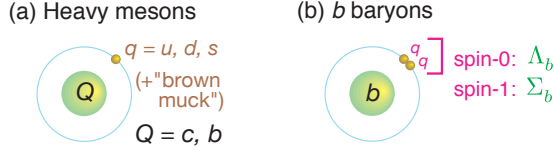


Fig. 5. (a) Atomic analogy of HQET for heavy mesons; (b) for bud, buu, bdd baryons.

5. Spectroscopy

5.1. B mesons

Heavy flavor spectroscopy provides the opportunity to test the theory of QCD bound states in the simplest system. Thus, heavy-quark hadrons can be considered the hydrogen atom of QCD, and b hadrons offer the heaviest quarks in bound systems. In the framework of Heavy Quark Effective Theory (HQET),¹⁰⁴ a b hadron can be roughly described by the heavier b quark being analogous to the nucleus of an atom with lighter u, d , or s quarks orbiting the nucleus similar to the electrons of an atom, but surrounded by a complicated, strongly interacting cloud of light quarks, antiquarks, and gluons sometimes referred to as “brown muck”¹⁰⁵ as shown in Fig. 5(a). Studies of these states provide very sensitive tests of potential models, HQET, and many regimes of QCD in general, including lattice gauge calculations and QCD strings.

The Tevatron has the capability of producing heavier states not accessible at the B factories running at the $\Upsilon(4S)$:

- bottom-strange mesons: B_s^0 ($\bar{b}s$, the ground state with the spins of the quarks anti-aligned) and B_s^* ($\bar{b}s$, with the spins of the quarks aligned);
- bottom-charm mesons B_c ($\bar{b}c$, the ground state);
- excited mesons B^{**} / B_s^{**} ($\bar{b}u, \bar{b}d$, and $\bar{b}s$ with the quarks having relative orbital angular momentum); and
- the b baryons Λ_b^0 (bud), $\Sigma_b^{(*)\pm}$ (buu and bdd), Ξ_b^- and Ξ_b^0 (bsd and bsu), and Ω_b^- (bss).

Using b hadron decay events with a J/ψ in the final state, CDF made what was at the time of publication the world’s best measurement¹⁰⁶ of the masses of the B^+ , B^0 , and B_s^0 mesons, as well as of the Λ_b^0 baryon. Fig. 6 shows the mass distributions for the various decay modes used in the analysis. The key to the measurement is a precise calibration of the momentum measurement for charged particles which is achieved using samples of $J/\psi \rightarrow \mu^+\mu^-$ and $\psi' \rightarrow J/\psi \pi^+\pi^-$ decays. In the study of spectroscopy, often it is the difference between particle masses that is most significant. That also has the advantage experimentally as many systematic uncertainties cancel. In the case of these measurements, the mass differences involving B_s^0 and Λ_b^0 were more precise than the existing world averages.

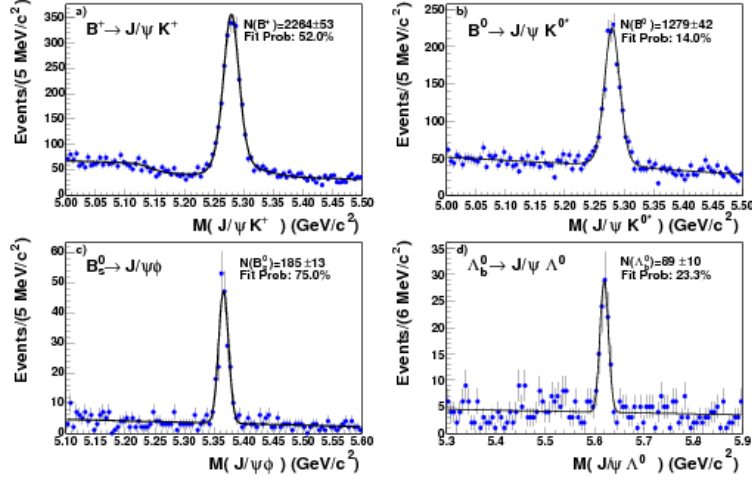


Fig. 6. The invariant mass distributions for $B^+ \rightarrow J/\psi K^+$, $B^0 \rightarrow J/\psi K^{*0}$, $B_s^0 \rightarrow J/\psi \phi$ and $\Lambda_b^0 \rightarrow J/\psi \Lambda^0$ candidates. The results of log-likelihood fits are superimposed. The fit probabilities obtained from a χ^2 test are shown.

The measured masses and differences are:

$$\begin{aligned}
 m(B^+) &= 5279.10 \pm 0.41 \text{ (stat)} \pm 0.36 \text{ (syst)} \text{ MeV}, \\
 m(B^0) &= 5279.63 \pm 0.53 \pm 0.33 \text{ MeV}, \\
 m(B_s^0) &= 5366.01 \pm 0.73 \pm 0.33 \text{ MeV}, \\
 m(B^+) - m(B^0) &= -0.53 \pm 0.67 \pm 0.14 \text{ MeV}, \\
 m(B_s^0) - m(B^0) &= 86.38 \pm 0.90 \pm 0.06 \text{ MeV}.
 \end{aligned}$$

B_c^+ mesons are predicted by the quark model to be members of the $J^P = 0$ pseudo-scalar ground-state multiplet and to have zero isospin as the lowest-lying bound state of a \bar{b} anti-quark and a c quark. This meson is of special interest because of its unique status as a short-lifetime bound state of heavy but different-flavor quarks. Measurements of its mass, production, lifetime (see Sect. 6.1), and decay (see Sect. 6.3) therefore allow for tests of theories under new approximation regimes or extended validity ranges beyond quarkonia which is formed from bound states of same-flavor quarks.

The CDF Collaboration made the first observation^{107, 108} of the B_c^+ meson in the fully reconstructed mode $B_c^+ \rightarrow J/\psi \pi^+$. Cuts on lifetime, momenta, resolutions, and other quantities were optimized in the topologically similar $B^+ \rightarrow J/\psi K^+$ sample. Fig. 7(a) shows the effect of the tight cuts on the background to the B^+ signal (inset) as well as the relative size of the B^+ and B_c^+ signals. The B_c^+ mass is determined in a binned log-likelihood fit and found to be $6275.6 \pm 2.9 \text{ (stat)} \pm 2.5 \text{ (syst)} \text{ MeV}$. The signal is observed with 8σ significance.

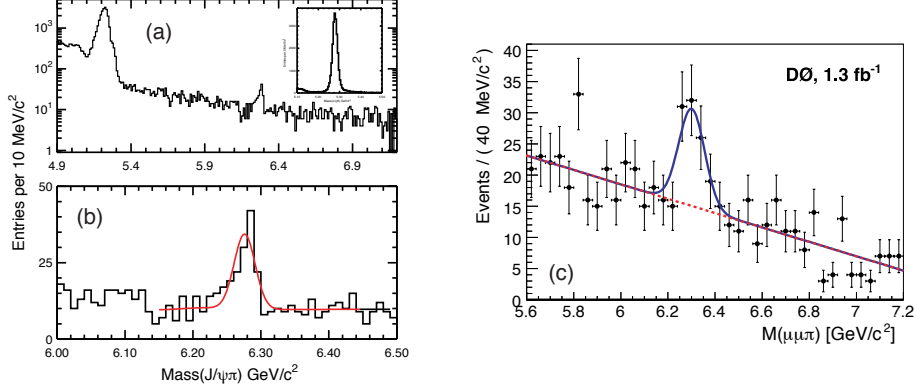


Fig. 7. (a) (inset) In CDF, the $J/\psi K^+$ mass distribution has an excellent signal-to-background ratio as a result of the optimized cuts. The $J/\psi \pi^+$ mass distribution shows a clear excess for the B_c^+ as well as the B^+ reflection; (b) the B_c^+ mass signal peak as determined in a binned likelihood fit; (c) $D\bar{O} B_c^+$ signal peak in the same channel.

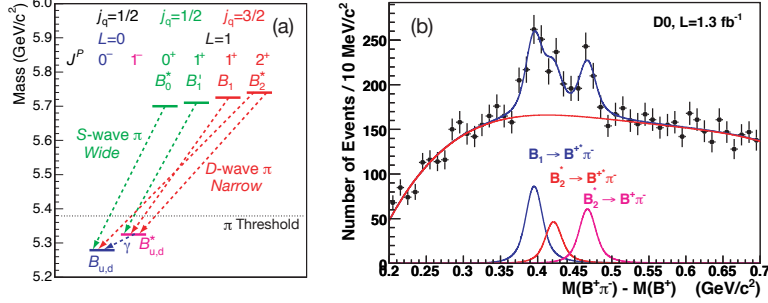


Fig. 8. (a) Spectroscopy of orbitally excited B meson states; (b) $D\bar{O}$ signal peaks for excited B meson states.

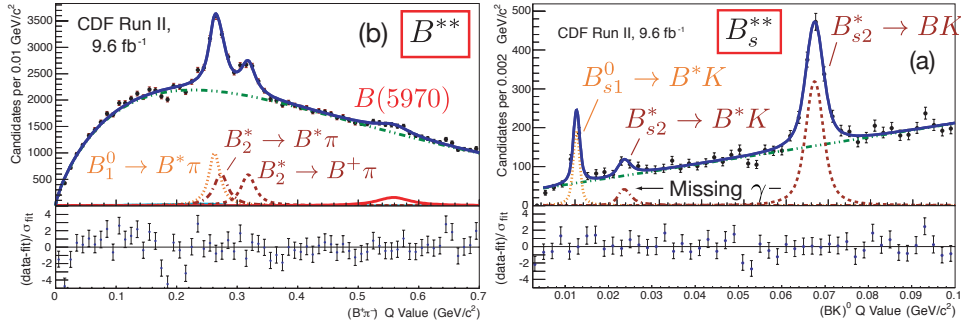
Using lifetime cuts and requiring a pion at large transverse momentum with respect to an identified $J/\psi \rightarrow \mu^+ \mu^-$, the $D\bar{O}$ Collaboration established a signal¹⁰⁹ shown in Fig. 7(b) for $B_c^+ \rightarrow J/\psi \pi^+$, with greater than 5σ significance and measured its mass to be 6300 ± 14 (stat) ± 5 (syst) MeV.

B^{**} and B_s^{**} mesons (also denoted B_J and $B_{s,J}$, respectively) are composed of a heavy b quark and a lighter u , d , or s quark in a $L = 1$ state of orbital momentum, with four possible states in each case as shown in Fig. 8(b), where only the two states that decay via D -wave transitions are narrow enough to be resolved above backgrounds. The mass splittings shown are analogous to the fine and hyperfine splittings in hydrogen.

By examining mass differences in the decay $B_J \rightarrow B^{(*)} \pi$, the $D\bar{O}$ Collaboration observed¹¹⁰ the B_1^0 and B_2^{*0} states for the first time as separated states (see Fig. 8(c) and measured their masses, mass splittings and production rates. The

Table 1. Measured masses and widths of $B_{(s)}^{**}$ mesons from CDF.

	Q (MeV)	Γ (MeV)
B_1^0	262.7 ± 0.9 $^{+1.1}_{-1.2}$	$23 \pm 3 \pm 4$
B_2^{*0}	317.9 ± 1.2 $^{+0.8}_{-0.9}$	22 $^{+3}_{-2}$ $^{+4}_{-5}$
B_1^+	262 ± 3 $^{+1}_{-3}$	49 $^{+12}_{-10}$ $^{+2}_{-13}$
B_2^{*+}	317.7 ± 1.2 $^{+0.3}_{-0.9}$	11 $^{+4}_{-3}$ $^{+3}_{-4}$
B_{s1}^0	$10.35 \pm 0.12 \pm 0.15$	$0.5 \pm 0.3 \pm 0.3$
B_{s2}^{*0}	$66.73 \pm 0.13 \pm 0.14$	$1.4 \pm 0.4 \pm 0.2$

Fig. 9. CDF (a) B_s^{**} (and radial excitation); and (b) B^{**} states ($Q = M(B^{**}) - M(B) - M(\pi^+)$).

CDF Collaboration in a similar analysis measured¹¹¹ the masses with higher precision and also measured the width of the B_2^{*0} for the first time. There are some discrepancies between the two measurements, the largest being a 2.7σ difference in the mass splittings between the two B^{**} states.

Similarly, searching for $B_{s2}^* \rightarrow B^+ K^-$ and $B_{s1}^* \rightarrow B^{*+} K^-$ decays, the CDF Collaboration reported¹¹² the first observation of the narrow $j_q \equiv s_q + L = 3/2$ states of the orbitally excited B_s^0 mesons with mass and mass splitting values consistent with theoretical predictions. The DØ Collaboration also observed¹¹³ the B_{s2}^* excited state but, given the data set at the time, was not able to make any conclusions about the presence of the B_{s1}^* .

Using the full Run 2 data set, the CDF Collaboration updated their measurements of the narrow orbitally excited states¹¹⁴ as shown in Fig. 9. The measurements include the masses and widths of the B_1 and B_2^* for all three meson flavors: B^{***} , B^{0**} , and B_s^{0**} . Fig. 9 shows the $B^- \pi^+$ and $B^- K^+$ mass distributions including the results of fits. The results are summarized in Table 1. This is the first observation of the B^{***} resonances. In addition, CDF observes an additional excess in both the charged and neutral channel at a $B\pi$ mass of approximately 5970 MeV with a width of about 70 MeV. The significance exceeds 4.4σ , and the mass is consistent with expectations for a radial excitation.

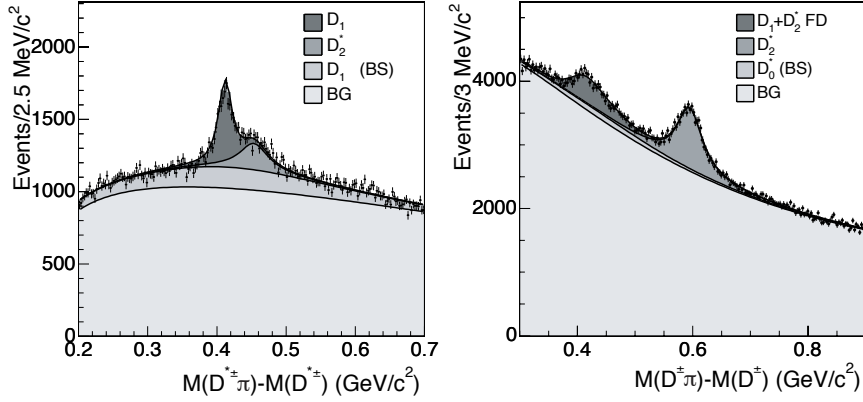


Fig. 10. Mass distributions for (a) $D^{*+}\pi^-$ and (b) $D^+\pi^-$ indicating the signals for D_1^0 and D_2^{*0} . In (b), the left peak arises from $D^{*+0} \rightarrow D^{*+}\pi^-$ decays where a π^0 from the D^* decay is not observed.

5.2. Charm mesons

Charm mesons display a similar set of excited states as described above for bottom mesons. While in the B system, decays to the B^* can be seen by a mass shift from the missing photon, in the charm system, isospin violation in D^* decays requires that the full final state be reconstructed. Absent efficient π^0 detection, measurements are limited to $D^{(*)+}\pi^-$ decays. CDF has measured¹¹⁵ masses and widths of the two neutral $j_q = 3/2$ states. The mass distributions for $D^+\pi^-$ and $D^{*+}\pi^-$ are shown in Fig. 10 where the various components of the fits are indicated showing clear signals for both the D_1^0 and D_2^{*0} ,

Using semileptonic decays of B mesons to orbitally excited charm states, the $D\mathcal{O}$ Collaboration has measured the masses of the D_1^0 and D_2^{*0} via the $B^0 \rightarrow D^{**}\mu\nu X$ decay¹¹⁶ and of the $D_{s1}^\pm(2536)$ via the $B_s^0 \rightarrow D_s^{**}\mu\nu X$ decay.¹¹⁷ The latter is particularly interesting given the surprisingly light masses of the $j_q = 1/2$ states plus the observation of new $D_{s,J}$ systems that may be quark molecular states.^{118,119}

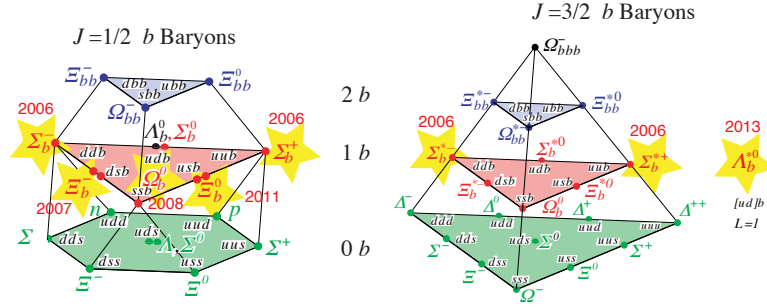
5.3. c and b -flavored baryons

In a continued analogy with atomic systems, baryons containing a b quark can be approximated as a heavy quark filling in for the nucleus orbited by a light diquark. Examples of the $L = 0$ system would then be the iso-singlet $J = 1/2$ Λ_b with the qq spins anti-aligned and the iso-triplet $J = 3/2$ Σ_b with the light quark spins aligned as shown in Fig. 5(b). Before Run 2 of the Tevatron, only the ground-state Λ_b had been identified, but the Tevatron has gone on to discover a host of new b baryons as shown in Fig. 11. With more data, the properties of these states were then measured with more precision.

Using the displaced track trigger samples, CDF made the first observation¹²⁰ with a significance of 5.2σ of the $\Sigma_b^{(*)}$ baryons in the decay mode $\Sigma_b^{(*)\pm} \rightarrow \Lambda_b^0\pi^\pm$

Table 2. CDF final results on masses of Ξ_c and b baryons.

Baryon	Mass (MeV/ c^2)
Ξ_c^0	$2470.85 \pm 0.24 \pm 0.55$
Ξ_c^+	$2468.00 \pm 0.18 \pm 0.51$
Λ_b	$5620.15 \pm 0.31 \pm 0.47$
Ξ_b^-	$5793.4 \pm 1.8 \pm 0.7$
Ξ_b^0	$5788.7 \pm 4.3 \pm 1.4$
Ω_b^-	$6047.5 \pm 3.8 \pm 0.6$
$M(\Xi_c^0) - M(\Xi_c^+)$	$2.85 \pm 0.30 \pm 0.04$
$M(\Xi_b^-) - M(\Xi_b^0)$	$4.7 \pm 4.7 \pm 0.7$

Fig. 11. Baryon multiplets with new b -flavored baryons discovered at the Tevatron indicated by the star symbols.

where $\Lambda_b^0 \rightarrow \Lambda_c^+ \pi^-$ and $\Lambda_c^+ \rightarrow p K^+ \pi^-$. With approximately four times more data, CDF refined their measurements¹²¹ and included measurements of the natural widths of each of the four charged Σ_b baryons (see Fig. 12(c)).

The DØ Collaboration, using 1.3 fb^{-1} of data, reported¹²² the first direct observation of the strange b baryon Ξ_b^- (bsd) via the fully reconstructed decay $\Xi_b^- \rightarrow J/\psi \Xi^-$ where $\Xi^- \rightarrow \Lambda^0 \pi^-$ (see Fig. 12(a)) and measured its mass and production rate with respect to $\Lambda_b^0 \rightarrow J/\psi \Lambda$. The CDF Collaboration also observed¹²³ this state. By reconstruction the trajectory of the Ξ^- in the silicon vertex detector, CDF was able to substantially decrease backgrounds and refine the Ξ^- momentum measurements. They measured a mass consistent with the DØ result, but with a significant improvement in precision. With additional data, CDF was able to extend the charged hyperon reconstruction technique to discover¹²⁴ the Ξ_b^0 in the decay mode $\Xi_b^0 \rightarrow \Xi_c^+ \pi^-$, $\Xi_c^+ \rightarrow \Xi^- \pi^+ \pi^+$ and measure its mass. This is a particle that could not be observed in a decay mode including J/ψ mesons that provide clean channels for other bottom particle discoveries at the Tevatron. In addition, CDF made the first observation of the decay mode $\Xi_b^- \rightarrow \Xi_c^0 \pi^-$, $\Xi_c^0 \rightarrow \Xi^- \pi^+$. As a by-product of the analyses that include fully reconstructed Ξ_c baryons, CDF has made the most precise measurements¹²⁵ of the Ξ_c^0 and Ξ_c^+ masses.

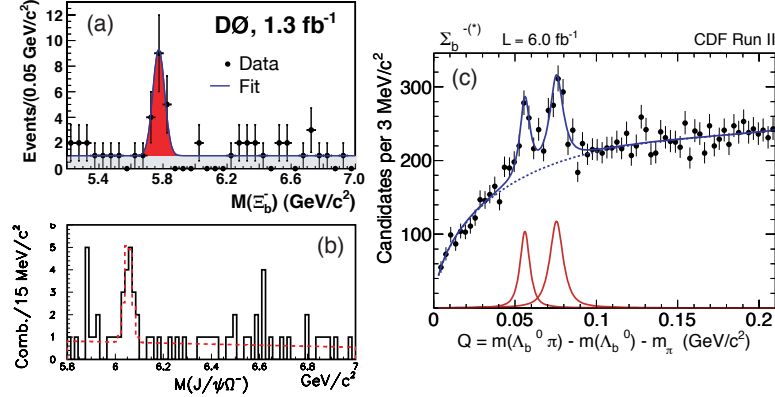


Fig. 12. (a) $D\Phi$ signal peak for $\Xi_b^\pm \rightarrow J/\psi \Xi$; (b) CDF signal peak for $\Omega_b \rightarrow J/\psi \Omega$; and (c) CDF updated signal peaks for Σ_b^- and Σ_b^{*-} .

In the decay mode of $\Omega_b^- \rightarrow J/\psi \Omega^-$, both the CDF (see Fig. 12(b)) and $D\Phi$ Collaborations reported observations^{126,127} of the doubly strange b baryon Ω_b^- (bss). The mass measurements of the Ω_b^- baryon were significantly different, $\Delta M = 111 \pm 12$ (stat) ± 14 (syst) MeV. Furthermore, CDF observed a substantially lower production rate relative to Ξ_b^- consistent with the $\sim 15\%$ expected for producing an additional $s\bar{s}$ pair while $D\Phi$ observed a relative rate close to unity. This CDF mass measurement, the updated mass measurement,¹²⁵ and a measurement from the LHCb Collaboration¹²⁸ are all consistent within small uncertainties. The $D\Phi$ Collaboration continues to investigate this signal with their full data set. CDF’s final results on Ξ_b and Ω_b masses and lifetimes using the full Run 2 dataset can be found in Ref. 125. The mass measurements are listed in Table 2.

CDF has also studied an excited state of a b baryon. The observation¹²⁹ of $\Lambda_b^{*0} \rightarrow \Lambda_b^0 \pi^+ \pi^-$, $\Lambda_b^{*0} \rightarrow J/\psi \Lambda^0$ with a significance of 3.5σ confirms the initial observation¹³⁰ made by LHCb. The mass splitting between Λ_b^{*0} and Λ_b^0 is $299.82 \pm 0.35 \pm 0.30$ MeV. Once again taking advantage of the displaced-track hadronic decay sample, CDF has measured¹³¹ the masses and widths of a variety of excited charm baryons in decay modes of the form $\Sigma_c^* \rightarrow \Lambda_c \pi$ and $\Lambda_c^* \rightarrow \Lambda_c \pi \pi$, which are typically the world’s most precise and provide important constraints on QCD models of baryon structure.

5.4. Exotic States

Starting with the discovery¹³² of a $J/\psi \pi^+ \pi^-$ resonance at around 3872 MeV by the Belle Collaboration in 2003, experimenters have uncovered a host of exotic charmonium-like particles with a variety of quantum numbers. The $X(3872)$, was first observed in exclusive decays $B^\pm \rightarrow X K^\pm$, $X \rightarrow J/\psi \pi^+ \pi^-$ from B mesons produced in $e^+ e^-$ collisions. The value of its mass very close to the $D^0 \bar{D}^{*0}$ mass threshold along with failure of models of conventional higher-mass $c\bar{c}$ charmonium

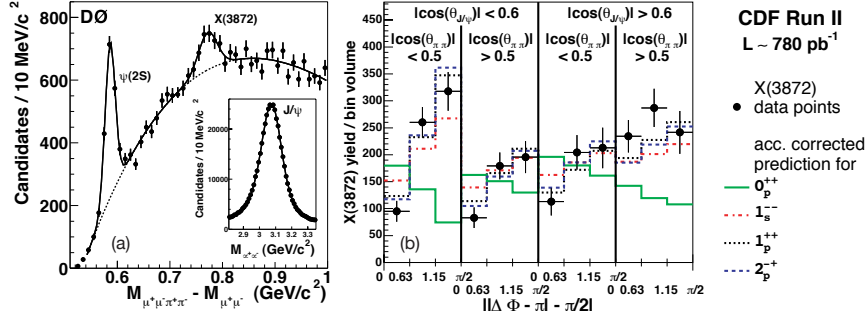
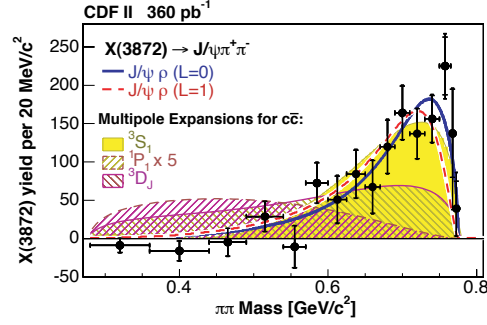
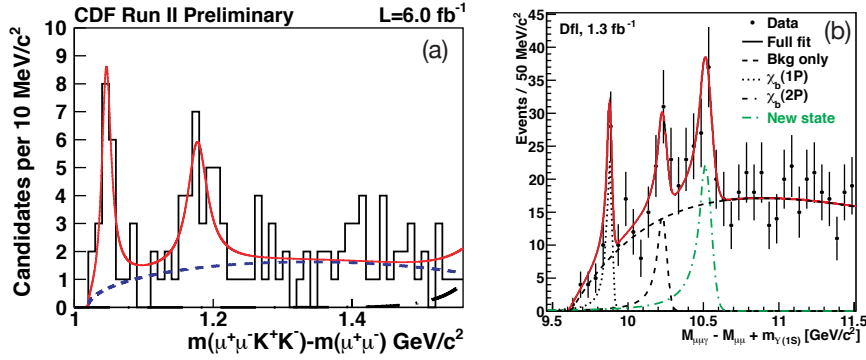


Fig. 13. (a) $D\bar{0}$ signal peak for $X(3872)$; (b) CDF angular analysis of the dipion system in $X(3872)$ decays.

states to match its mass has generated a great deal of interest in this state, with suggestions of it being a weakly bound $D^0\bar{D}^{*0}$ “molecular” state,¹³³ a possible four-quark state,¹³⁴ or a $c\bar{c}g$ hybrid.

Shortly following this discovery, both the CDF and $D\bar{0}$ Collaborations also observed^{135, 136} inclusive production of this narrow state in $p\bar{p}$ collisions through the decay $X(3872) \rightarrow J/\psi \pi^+\pi^-$ as shown in Fig. 13(a). $D\bar{0}$ compared characteristics of the decay with that of the $\psi(2S)$ and observed no differences,¹³⁶ while CDF, with larger data sets, made more detailed measurements of its properties. One hypothesis for the $X(3872)$ is that it is a four-quark state. Therefore, there would be two different states $c\bar{c}u\bar{u}$ and $c\bar{c}d\bar{d}$ with slightly different masses.¹³⁴ CDF placed an upper limit¹³⁷ of 3.6 MeV for the mass splitting of the two states assuming equal abundance, effectively excluding the four-quark hypothesis. Given that the $X(3872)$ is a single narrow state, CDF then made the most precise measurement of its mass: $3871.61 \pm 0.16 \pm 0.19$ MeV. A CDF study¹³⁸ of the dipion mass distribution placed constraints on its J^{PC} assignment. Fig. 14 compares the observed dipion mass spectrum to the lowest C -odd possibilities. The data give a good fit to $J/\psi\rho^0$ models, but it is not possible to differentiate between $J = 0$ and $J = 1$. To determine the spin-parity of the state, CDF used a larger data sample and performed an angular analysis as shown in Fig. 13(b) where the fit clearly favors the $J/\psi\rho^0$ hypothesis, but finds $J^{PC} = 1^{++}$ and 2^{-+} to be equally likely, each with a χ^2 probability of 28%.

In 2009, the CDF Collaboration reported¹³⁹ evidence of a narrow structure near the $J/\psi\phi$ threshold in exclusive $B^+ \rightarrow J/\psi\phi K^+$ decays and measured its mass and width. This state does not fit conventional expectations for charmonium which above the threshold for open charm decays should decay predominantly to a pair of charm particles rather than to $J/\psi\phi$. This anomalous state, known as $Y(4140)$ has been given theoretical interpretations similar to those for $X(3872)$.¹⁴⁰ The $D\bar{0}$ Collaboration has confirmed¹⁴¹ (calling it the $X(4140)$) this enhancement at greater than 3σ significance. Observation¹⁴² by the CMS Collaboration supports

Fig. 14. CDF fit to the dipion mass distribution in $X(3872)$ decays.Fig. 15. (a) CDF signal peak for $Y(4140)$; and (b) $D\bar{D}$ peaks for decays into $\Upsilon(1S)\gamma$.

the Tevatron measurements. Belle has searched for $Y(4140)$ state and observes¹⁴³ no signal, although does not rule it out, while LHCb has searched for the state and has also observed¹⁴⁴ no evidence, in disagreement with the CDF result at the 2.4σ level.

Discoveries of more b -quark counterparts to the possible exotic states above could shed light on their underlying structure. The $D\bar{D}$ Collaboration has searched for particles decaying into $\Upsilon(1S) + \gamma$ and observes¹⁴⁵ the $\chi_b(1P)$, $\chi_b(2P)$, plus a third higher-mass structure (see Fig. 15(b)) consistent with a state observed¹⁴⁶ by the ATLAS Collaboration. Further analysis is needed to determine whether this structure is due to the $\chi_b(3P)$ system or some exotic b -quark state.

Models^{147,148} of supersymmetry that include light scalar quarks would include bound states that decay to dimuons similarly to quarkonium. CDF searched¹⁴⁹ for narrow states below the Υ . By comparing to the $\Upsilon(1S) \rightarrow \mu^+\mu^-$ yield, CDF is able to set limits in a sample of 630 pb^{-1} on narrow resonances in the range

$6.3 < M_{\mu\mu} < 9.0 \text{ GeV}$, excluding models with 1^{--} bound states in that mass region.

6. Decays and Lifetimes

Precision lifetime measurements of b hadrons are needed in the extraction of the weak parameters that are important for understanding the role of the CKM matrix throughout heavy flavor physics, including from CP violation. In the simplest spectator model for weakly decaying b hadrons, there is only the flavor-changing direct $b \rightarrow Wq$, ($q = c, u$) decay, without any involvement or interactions with the other anti-quark in a B meson or quarks in a b baryon, and the lifetimes of all b hadrons would be identical. Non-spectator effects, such as W exchange and the interference between contributing amplitudes, modify this simple picture and give rise to a lifetime hierarchy for b hadrons similar to the one observed for charm hadrons, although variations are expected to be smaller since lifetime differences are expected to scale as $1/m_Q^2$. The expected hierarchy is:

$$\tau(B^+) \geq \tau(B^0) \simeq \tau(B_s^0) > \tau(\Lambda_b^0) \gg \tau(B_c^+). \quad (2)$$

Lifetime differences thus test our understanding of quark dynamics in b hadrons with comparisons to predictions of heavy quark expansions (HQE).^{150,151}

6.1. B meson lifetimes

Despite the huge samples of B^0 and B^+ mesons at the $\Upsilon(4S)$ B factories, the Tevatron experiments' measurements of $\tau(B^0)$ and $\tau(B^+)$, including their ratio, were the best in the world prior to the first results from LHCb, with a precision of better than 1%. These measurements are also important benchmarks for measuring the lifetimes of the heavier b hadrons at the Tevatron.

Both the CDF and $D\bar{O}$ Collaborations have measured^{152–157} $\tau(B^0)$ and $\tau(B^+)$ through the exclusive decays $B \rightarrow J/\psi K$, including when ratios are made to other lifetimes. The $D\bar{O}$ Collaboration also measured the ratio $\tau(B^+)/\tau(B^0)$ by examining the time evolution of the number of $B^+ \rightarrow \bar{D}^0 \mu^+ \nu X$ decays compared to $B^0 \rightarrow D^{*-} \mu^+ \mu X$ decays. CDF has measured¹⁵⁸ the B^+ lifetime in the decay mode $B^+ \rightarrow \bar{D}^0 \pi^+$ with data from the displaced hadron trigger using a novel technique that accounts for the decay-time bias of the trigger without simulation.

Neutral B mesons contain short- and long-lived components, since their light (L) and heavy (H) eigenstates, B_L and B_H , differ not only in their masses, but also in their total decay widths, with a decay width difference defined as $\Delta\Gamma = \Gamma_L - \Gamma_H$. Neglecting CP violation in B - \bar{B} mixing, which is expected to be very small, the mass eigenstates are also CP eigenstates with the light B_L state being CP -even and the heavy B_H state being CP -odd. While the decay width difference $\Delta\Gamma_d$ is tiny and can be neglected in the B^0 system, the B_s^0 system exhibits a significant value of $\Delta\Gamma_s$ with $\Delta\Gamma_s/\Gamma_s \simeq 10\%$. For the B_s^0 meson, the mean lifetime, defined as

$1/\Gamma_s$ where $\Gamma_s = (\Gamma_{sL} + \Gamma_{sH})/2$, and $\Delta\Gamma_s$ are the fundamental parameters, and the measured lifetime will depend on the final state.

By isolating the decay $B_s^0 \rightarrow J/\psi f_0(980)$, the CDF Collaboration made the first measurement¹⁵⁹ of the B_s^0 lifetime with a CP -eigenstate as a final state, thus directly determining $1/\Gamma_H = 1/(\Gamma_s - \Delta\Gamma_s/2)$ (neglecting CP violation).

Flavor-specific decays, such as semileptonic $B_s^0 \rightarrow D_s^- \ell^+ \nu$ or $B_s^0 \rightarrow D^- \pi^+$ have equal fractions of B_L and B_H at time $t = 0$. If the resulting superposition of two exponential distributions is fitted with a single exponential function, one measures the flavor-specific lifetime from which Γ_s and $\Delta\Gamma_s$ can be extracted (see Ref. 160). Using an exclusive final state $B_s^0 \rightarrow D_s^- \pi^+$, the CDF Collaboration measured¹⁶¹ the flavor-specific lifetime. The DØ Collaboration measured¹⁶² what was at that time the world's best flavor-specific lifetime in the semileptonic mode $B_s^0 \rightarrow D_s^- \mu^+ \nu X$, finding the boost by correcting for the missing neutrino energy using correction distributions determined by MC.

The final state in the decay $B_s^0 \rightarrow J/\psi \phi$ contains a mixture of CP -even and CP -odd components. Early analyses^{152,163} focused on measuring the effective single lifetime of this decay channel, and the CDF Collaboration performed the first analysis¹⁶⁴ that separated the two CP components through a full angular study to determine directly $1/\Gamma_s$ and Γ_s . Subsequent analyses by both CDF and DØ focusing on extracting $\Delta\Gamma_s$ specifically, and then including the CP -violating phase in B_s^0 mixing and are discussed in more detail in Sections 7 and 8.3, respectively.

For the B_c^+ meson, both quarks decay weakly, so the lifetime is expected to be much shorter. Early measurements of the B_c^+ meson lifetime, from CDF¹⁶⁵ and DØ,¹⁶⁶ use the semileptonic decay mode $B_c^+ \rightarrow J/\psi \ell X$ and are based on a simultaneous fit to the mass and lifetime using as a decay point the vertex formed with the leptons from the decay of the J/ψ and a third lepton. Because the B_c^+ decay is not fully reconstructed, these analyses require significant background subtractions and correction factors to estimate the boost due to the missing neutrino. The recent determination¹⁶⁷ of the B_c^+ lifetime, from the CDF Collaboration is based on fully reconstructed $B_c^+ \rightarrow J/\psi \pi^+$ decays. Notwithstanding the limitations of the semileptonic measurements, for a given luminosity, they still have significantly better resolution resulting from the much larger sample sizes. The Tevatron average of these measurements is $\tau(B_c^+) = 0.458 \pm 0.030$ ps, significantly shorter, as expected, than the approximately 1.5 ps lifetime of the other b hadrons.

6.2. b baryon lifetimes

The ratio $\tau(\Lambda_b^0)/\tau(B^0)$ has gained a great deal of attention since predictions of this ratio ranged from above 0.90 to only being a few percent below unity,^{151,168} whereas in the early 2000's, the average value was far below this prediction, with an experimental world average¹⁶⁹ in 2002 being 0.800 ± 0.081 (and 0.786 ± 0.034 for a b -baryon mixture). The DØ Collaboration has measured¹⁷⁰ this lifetime in the semileptonic mode $\Lambda_b^0 \rightarrow \Lambda_c^+ \mu^- \nu X$, and CDF has measured¹⁷¹ the lifetime in the

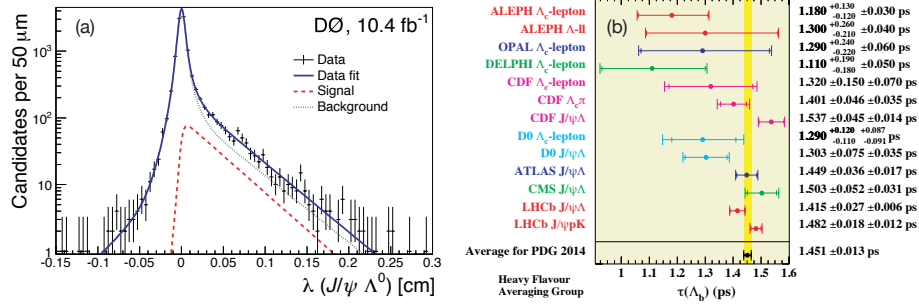


Fig. 16. (a) Decay length distribution for $\Lambda_b^0 \rightarrow J/\psi \Lambda$ decays in $D\bar{D}$. (b) Measurements of $\tau(\Lambda_b^0)$.

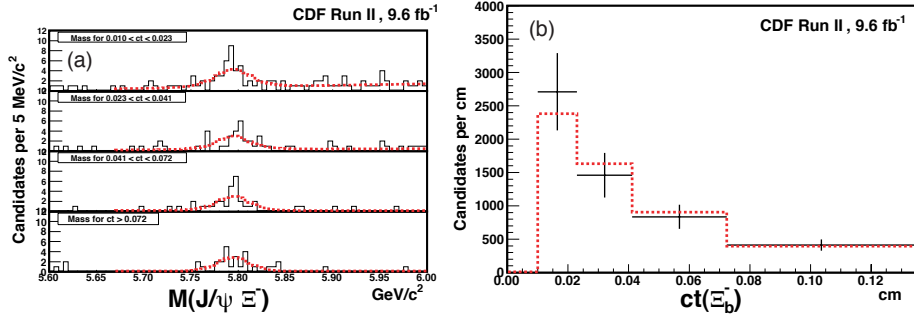


Fig. 17. (a) Mass distributions of $J/\psi \Xi^-$ in four bins of proper decay time from CDF. The red dotted line shows the result of an unbinned likelihood fit for the Ξ_b^- yield. (b) Lifetime distribution using the yields from the fits to the mass distributions. The red dashed line shows the fit for the Ξ_b^- lifetime.

exclusive mode $\Lambda_b^0 \rightarrow \Lambda_c^+ \pi^-$, while both collaborations have measured^{125, 154–157, 172} it via $\Lambda_b^0 \rightarrow J/\psi \Lambda^0$ with an example of a fit to the decay length distribution shown in Fig. 16(a). The evolution of measurements of $\tau(\Lambda_b^0)$ can be seen in Fig. 16(b), where the world average lifetime has now been pulled higher, with Tevatron measurements being consistent with each other, the current world average, and current theoretical predictions.

CDF has measured^{125, 126} the lifetime of the Ξ_b^- and Ω_b^- baryons in the decay modes $\Xi_b^- \rightarrow J/\psi \Xi^-$, $\Xi^- \rightarrow \Lambda^0 \pi^-$ and $\Omega_b^- \rightarrow J/\psi \Omega^-$, $\Omega^- \rightarrow \Lambda^0 K^-$ where the charged hyperons are tracked in the silicon detector as described in Section 5.3. The lifetime is determined by measuring the yield in $J/\psi \Xi^-$ or $J/\psi \Omega^-$ mass distributions for several regions of proper time and then fitting the derived proper time distribution for the lifetime. The results for Ξ_b^- are shown in Fig. 17.

6.3. Decay modes and branching ratios

In many cases, specific branching fractions are measured along the road to other results, such as CP violation and precise measurements of neutral B meson mixing parameters, or in the process of exploring the properties of one of final-state particles, using the final state of b -hadron decays to provide a clean sample.

The DØ Collaboration has investigated¹¹⁶ the properties of semileptonic decays of B^0 mesons to orbitally excited states of the D meson that have small decay widths, *i.e.*, those that decay via D -wave transitions. Using mild assumptions on the subsequent branching fractions of the excited mesons D_1 and D_2^* , world's-best measurements of the branching fractions $\mathcal{B}(B \rightarrow \bar{D}_1^0 \ell^+ \nu X)$ and $\mathcal{B}(B \rightarrow \bar{D}_2^{*0} \ell^+ \nu X)$ were made along with the first measurement of their ratio R , one of the least model-dependent predictions^{173,174} of HQET for these states. Similarly, DØ made a first measurement¹¹⁷ of the branching fraction of $\mathcal{B}(B_s^0 \rightarrow D_{s1}^-(2536) \mu \nu_\mu X)$, while providing measurements of the properties of the $D_{s1}^-(2536)$, as described in Sect. 5.2.

In preparation for CP -violation measurements, both the CDF and DØ Collaborations measured^{152,164} the linear polarization amplitudes in the decay $B^0 \rightarrow J/\psi K^{*0}$, and measurements of the strong phases indicated evidence for the presence of final-state interactions for this decay. Comparisons with same measurements in the analogous decay $B_s^0 \rightarrow J/\psi \phi$ were consistent with SU(3) symmetry, *i.e.*, that the strong phases are consistent with being the same in both systems.

The study of B meson decays into several charmonium states can also be used to constrain the long-distance parameters associated with color-octet production which are important for the understanding of both mixing induced and direct CP violation. It also allows for possible additional channels, and provides a test of quark-hadron duality in the comparison with B^0 and B^+ decays. Both the CDF and DØ Collaborations have measured^{175,176} the ratio of branching fractions of $B_s^0 \rightarrow \psi' \phi$ to $B_s^0 \rightarrow J/\psi \phi$ to be consistent with the ratio of branching fractions of $B^\pm \rightarrow \psi' K^\pm$ to $B^\pm \rightarrow J/\psi K^\pm$.

The decay products in $B_s^0 \rightarrow J/\psi f_0(980)$ are in a CP -odd eigenstate, which can provide a more direct measurement of the CP -violating phase ϕ_s as compared to the decay $B_s^0 \rightarrow J/\psi \phi$ where the decay products are in an indefinite CP state (see Sect. 8). This can provide a useful additional channel, although the branching fraction of the former is expected to be smaller. Also, the decay chain $B_s^0 \rightarrow J/\psi f_0(980), f_0(980) \rightarrow K^+ K^-$ forms a background to $B_s^0 \rightarrow J/\psi \phi$ that must be constrained in studies of CP violation. The CDF and DØ Collaborations measured^{159,177} the ratio of the $B_s^0 \rightarrow J/\psi f_0(980)$ and $B_s^0 \rightarrow J/\psi \phi$ branching fractions to be consistent with expectations.

$B_s^0 \rightarrow J/\psi K_S^0$ is a CP eigenstate, and measurement of its lifetime would directly probe the lifetime $\tau_{B_{sH}}$. Additionally, large samples can be used to extract the angle γ of the unitary triangle. CDF made the first observation¹⁷⁸ of the Cabibbo-suppressed decay modes $B_s^0 \rightarrow J/\psi K_S^0$ and $B_s^0 \rightarrow J/\psi K^{*0}$, observing both with greater than 7σ significance.

The DØ Collaboration studied¹⁷⁹ the decays $B_s^0 \rightarrow J/\psi K^+ K^-$, and from the invariant mass and spin of the $K^+ K^-$ system, found evidence for the two-body decay $B_s^0 \rightarrow J/\psi f_2'(1525)$ and measured the relative branching fraction of the decays with respect to the rate into $J/\psi \phi$.

In Run 2, CDF made the first studies of hadronic decays of B_s^0 mesons. Taking advantage of the samples and techniques developed for the measurement of B_s^0 mixing (Sect. 7.3), CDF measured¹⁸⁰ the ratios of branching fractions $B(B_s^0 \rightarrow D_s^- \pi^+ \pi^+ \pi^-)/B(B^0 \rightarrow D^- \pi^+ \pi^+ \pi^-)$ and $B(B_s^0 \rightarrow D_s^- \pi^+)/B(B^0 \rightarrow D^- \pi^+)$

In studies of decay modes that can be used for future studies of CP violation, the DØ Collaboration reported the first evidence^{181,182} for the decay $B_s^0 \rightarrow D_s^{(*)-} D_s^{(*)0}$ with CDF quickly following with the first observation¹⁸³ of the decay $B_s^0 \rightarrow D_s^+ D_s^-$ with a 7.5σ significance and measured its branching ratio. Subsequently, CDF made the world's best measurements¹⁸⁴ of the $B_s^0 \rightarrow D_s^{(*)+} D_s^{(*)-}$ branching ratios. These modes are also important as they can be used to measure lifetimes of the CP -even eigenstate of B_s^0 that complements the measurements of the CP -odd state $B_s^0 \rightarrow J/\psi f_0(980)$. In another mode with potential for future CPV studies, CDF made the first observation¹⁸⁵ of $\bar{B}_s^0 \rightarrow D_s^\pm K^\mp$ and measured the ratio of branching fraction relative to that for $\bar{B}_s^0 \rightarrow D_s^+ \pi^-$.

CDF also made great strides in the studies of hadronic decays of b baryons, making the first observation¹⁸⁶ of a fully hadronic Λ_b^0 decay and measuring the ratio of cross section times branching ratio for the mode $\Lambda_b^0 \rightarrow \Lambda_c^+ \pi^-$ relative to $\bar{B}^0 \rightarrow D^+ \pi^-$. More data brought the ability to do detailed analysis of baryon decays including a measurement¹⁸⁷ of the branching fraction $\mathcal{B}(\Lambda_b^0 \rightarrow \Lambda_c^+ \pi^- \pi^+ \pi^-)$ including of the resonant substructure of this multibody decay mode.

7. Mixing and Oscillations of Heavy Neutral Mesons

Neutral meson systems exhibit the phenomenon of particle-antiparticle oscillations that can proceed by a second-order weak box diagram as shown in Fig. 18(a). The intense interest in this process is due to the access provided to CKM matrix elements (e.g., V_{td} and V_{ts}), as well as probing for new heavy particles that could also be participate in the box diagram. The time evolution for a meson M of such a M^0 - \bar{M}^0 system is then governed by 2×2 mass and decay matrices. In each of these systems, the light (L) and heavy (H) mass eigenstates,

$$|M_{L,H}\rangle = p|M^0\rangle \pm q|\bar{M}^0\rangle, \quad (3)$$

have a mass difference $\Delta m = m_H - m_L$ and a decay width difference $\Delta\Gamma = \Gamma_L - \Gamma_H$ with values determined by the off-diagonal terms of the mass and decay matrix. We further define $x = \Delta m/\Gamma$ and $y = \Delta\Gamma/2\Gamma$, where $\Gamma = (\Gamma_L + \Gamma_H)/2$. In the absence of CP violation in the mixing, $|q/p| = 1$. Neglecting CP violation, the probability density \mathcal{P}_+ (\mathcal{P}_-) for a \bar{M}^0 produced at proper time $t = 0$ to decay as a \bar{M}^0 (M^0) at time t is then

$$\mathcal{P}_\pm(t) = \frac{\Gamma}{2} e^{-\Gamma t} [1 \pm \cos(\Delta m_q t)]. \quad (4)$$

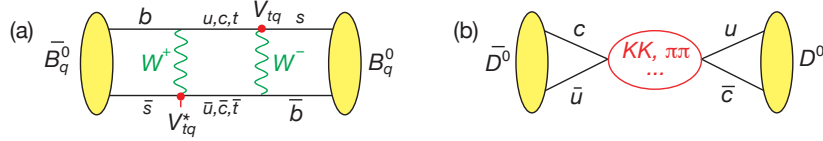


Fig. 18. (a) Example of second-order box diagram responsible for neutral meson mixing, in this case for neutral B mesons with $q = d, s$. (b) Long-range contribution for charm mixing.

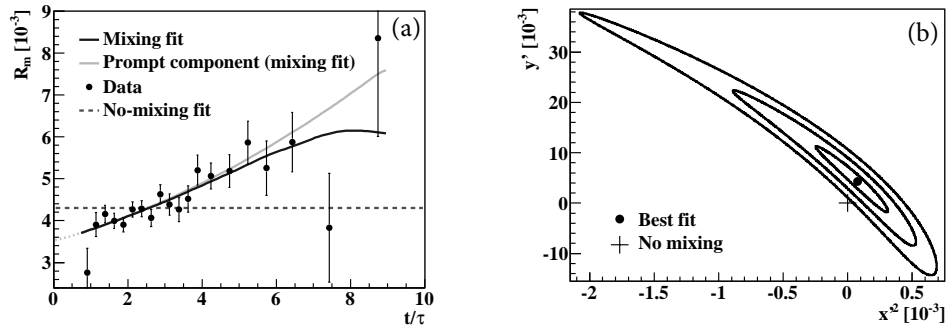


Fig. 19. (a) Measured ratio R_m of wrong-sign to right-sign D^0 decays as a function of normalized proper decay time. The results of a least-squares fit are shown for the mixing fit and for the prompt component. A fit assuming no mixing is clearly incompatible with the data. (b) Contours in x'^2 - y' parameter space bounding regions with Bayesian posterior probability corresponding to 1, 3, and 5 Gaussian standard deviations.

7.1. Charm mixing

In the standard model, D^0 - \bar{D}^0 mixing is a weak interaction process that occurs primarily through long-range virtual intermediate states that consist of common decay channels for particle and antiparticle, such as $\pi^+\pi^-$ (see Fig. 18(b).) Mixing could also result from exotic particles that appear as virtual states in a short-range box diagram. The decay $D^0 \rightarrow K^+\pi^-$ can arise from mixing of a D^0 state to a \bar{D}^0 state, followed by a Cabibbo-favored (CF) decay, or from a doubly Cabibbo-suppressed (DCS) decay of a D^0 . Several experiments have measured^{188–190} the ratio R of $D^0 \rightarrow K^+\pi^-$ to $D^0 \rightarrow K^-\pi^+$ decay rates and have seen 3σ evidence for mixing. R can be approximated¹⁰⁰ as a quadratic function of t/τ , where t is the proper decay time and τ is the mean D^0 lifetime:

$$R(t/\tau) = R_D + \sqrt{R_D}y'(t/\tau) + \frac{x'^2 + y'^2}{4}(t/\tau)^2, \quad (5)$$

where R_D is the squared modulus of the ratio of DCS to CF amplitudes, $x' = x \cos \delta + y \sin \delta$ and $y' = -x \sin \delta + y \cos \delta$, x and y are defined as above, and δ is the strong-interaction phase difference between the DCS and CF amplitudes. In the absence of mixing, $x = y = 0$ and $R(t/\tau) = R_D$.

Following first $> 5\sigma$ observation¹³⁰ of D^0 mixing by LHCb, CDF confirmed¹⁹¹

the effect, observing mixing with 6σ significance. The deviation of $R(t/\tau)$ from a constant is clearly visible in Fig.19(a) which shows the data as well as the results of a fit to Eq. 5, while Fig. 19(b) shows contours for the values of x'^2 and y' returned by the fit.

7.2. B^0 mixing and oscillations

The identification of B^0 oscillations and extraction of Δm_d use Eq. 4 and the measurement of probability density functions that describe the measured time development of B^0 mesons that decay with the same or opposite flavor as their flavor at production. The flavor, *i.e.* B^0 or \bar{B}^0 , at the time of decay is determined by the charge of the decay products. Since the dominant production mechanisms at the Tevatron produce $b\bar{b}$ pairs, the flavor at the time of production can be determined by the charge of the lepton from semileptonic decays or a momentum-weighted charge of the decay products of the second b hadron produced in the collision.

Since B^0 oscillations were definitively measured at the B factories, measurements at the Tevatron, *e.g.* by the $D\bar{O}$ Collaboration¹⁹² were mostly pursued as controls comparing to the world average value (currently $\Delta m_d = 0.507 \pm 0.004 \text{ ps}^{-1}$) in preparation for searching for B_s^0 oscillations and to calibrate the tagging power of flavor-tag techniques. A measurement of $\Delta\Gamma_d/\Gamma_d = 0.0079 \pm 0.0115$ has been made at the Tevatron by $D\bar{O}$,¹⁹³ as described in Sect. 8.3.

7.3. B_s^0 mixing and oscillations

The determination of the the B_s^0 - \bar{B}_s^0 oscillation frequency Δm_s has been a major goal of experimental particle physics since the first observation of B^0 mixing in 1987.^{194,195} Since $|V_{ts}|$ is larger than $|V_{td}|$, the oscillation frequency Δm_s was expected to be much greater than that for B^0 - \bar{B}^0 oscillations, requiring the large data samples and excellent proper time resolution available at the Tevatron and its detectors. In addition to the opposite-side tagging described above, same-side tagging was also used to take advantage of fragmentation on the reconstructed side of the event. For an example, if an associated K^+ containing a strange antiquark is found, the strange quark will have likely hadronized with a \bar{b} , tagging the flavor at production

Until the Tevatron Run 2 started, there were only lower limits on the value of Δm_s . The $D\bar{O}$ Collaboration placed¹⁹⁶ the first two-sided limit (at 90% C.L.) on Δm_s (see Fig. 20). Shortly after, the CDF Collaboration made the first $>5\sigma$ observation of B_s^0 - \bar{B}_s^0 oscillations and the first measurement¹⁹⁷ of Δm_s . A follow-up publication¹⁹⁸ from CDF with subsequent improvements then reported a measurement of

$$\Delta m_s = 17.77 \pm 0.10 \text{ (stat)} \pm 0.07 \text{ (sys)} \text{ ps}^{-1}, \quad (6)$$

as shown in Fig. 20(b,c).

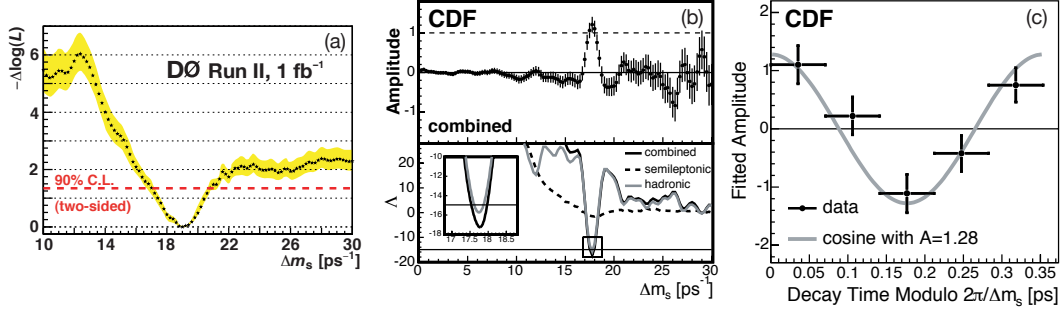


Fig. 20. (a) Result of a $D\bar{0}$ likelihood analysis¹⁹⁶ showing $\Delta \log \mathcal{L}$ as a function of Δm_s ; (b) measured amplitude values and uncertainties (upper) and the logarithm of the ratio of likelihoods for amplitude equal to one and amplitude equal to zero for the CDF result;¹⁹⁷ and (c) for the same analysis, the oscillation signal measured in five bins of proper decay time modulo the measured oscillation period.

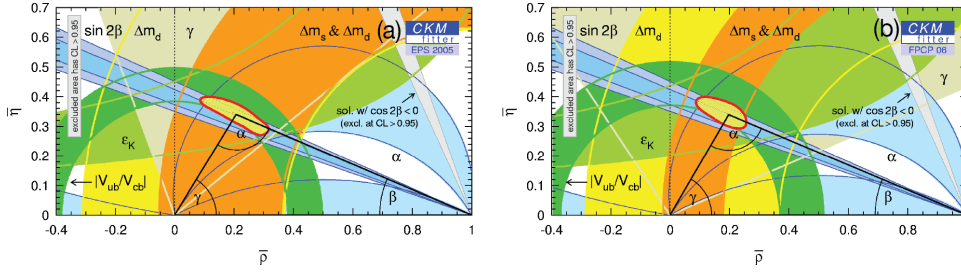


Fig. 21. Constraints on the apex $(\bar{\rho}, \bar{\eta})$ of the B -meson CKM unitarity triangle (a) before and (b) after the Tevatron result on Δm_s . From Ref. 199 (see for definition of $\bar{\rho}$ and $\bar{\eta}$).

An important goal of heavy flavor physics is constraining the CKM matrix using experimental results on observables together with theoretical inputs and unitarity conditions. The constraint from our knowledge on the ratio $\Delta m_s/\Delta m_d$ and hence $|V_{td}/V_{ts}|$ is more effective in limiting the position of the apex of the CKM B -meson unitarity triangle than the one obtained from Δm_d measurements alone, due to the reduced hadronic uncertainty as shown comparing constraints on the CKM matrix in Fig. 21(a) before and (b) after the measurement of Δm_s from the Tevatron.¹⁹⁹ The measured value of Δm_s is also consistent with the Standard Model prediction at the time of $\Delta m_s = 19.0 \pm 1.5 \text{ ps}^{-1}$ obtained²⁰⁰ from CKM fits where no experimental information on Δm_s is used.

The existence of final states to which both the B_s^0 and \bar{B}_s^0 can decay, such as $B_s^0 \rightarrow D_s^+ D_s^-$ and $B_s^0 \rightarrow J/\psi \phi$ which involve $b \rightarrow c\bar{c}s$ transitions, results in a relatively large value of the width difference between mass eigenstates $\Delta\Gamma_s/\Gamma_s \simeq 10\%$. In contrast the $b \rightarrow c\bar{c}d$ transition is Cabibbo-suppressed so that $\Delta\Gamma_d/\Gamma_d$ is

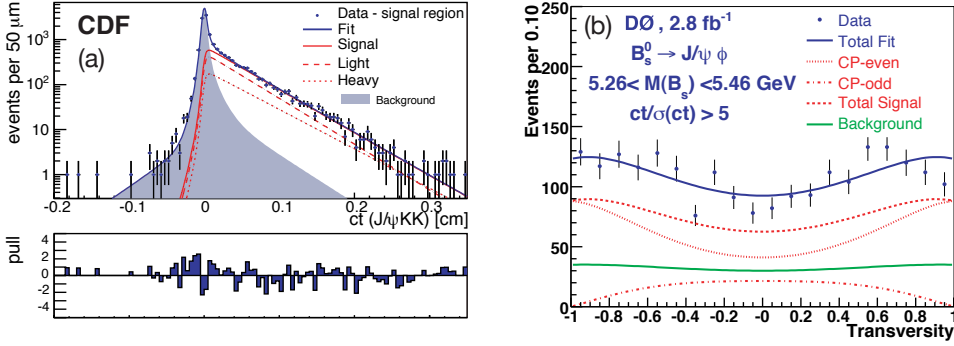


Fig. 22. (a) Example of a proper decay time fit projections for light and heavy mass eigenstates from a CDF analysis²⁰⁹ (6.5 fb^{-1}); and (b) example of fit to transversity angle of the μ^+ in the J/ψ rest frame with respect to the ϕ decay plane to CP -even (“light”) and CP -odd (“heavy”) components from a $D\bar{O}$ analysis²⁰⁴ (2.8 fb^{-1}).

tiny in the standard model. The large value of $\Delta\Gamma_s$ allows for an additional richness of physics in the B_s^0 system.

Because other CP eigenstate decay modes are either helicity or CKM suppressed, then under certain theoretical assumptions²⁰¹ the semi-inclusive decays $B_s^0 \rightarrow D_s^{(*)} D_s^{(*)}$ saturate the CP -even eigenstates in the B_s^0 . Thus the partial width for this mode accounts for the difference between the widths of B_{sL} and B_{sH} and $\Delta\Gamma_s^{\text{CP}}$ can be measured using information from branching ratios without lifetime fits.²⁰² The branching fraction^{181–184} measurements by CDF and $D\bar{O}$ described in Sec. 6.3 can be used to find $\Delta\Gamma_s^{\text{CP}} = \Delta\Gamma_s / \cos\phi_s$, where ϕ_s is the CP -violating mixing phase (see Sect.8) that can constrain models of new physics.

Determinations of $\Delta\Gamma_s$ and Γ_s in specific CP eigenstates were discussed in Sect. 6.1. The best sensitivity to $\Delta\Gamma_s$ and Γ_s (and hence the for the mean lifetime $\tau(B_s^0) = 1/\Gamma_s$) is achieved by time-dependent measurements of the $B_s^0 \rightarrow J/\psi \phi$ decay where the CP -even and CP -odd components are separated via a full angular analysis of the $J/\psi \rightarrow \mu^+ \mu^-$ and $\phi \rightarrow K^+ K^-$ decay products. Fit projections from two analyses are shown in Fig. 22. Both untagged and flavor-tagged analyses have been pursued at the Tevatron, with earlier analyses assuming no CP violation and then being optimized to measure the CP -violating phase ϕ_s . A complication is the possibility of a S -wave $K^+ K^-$ amplitude in addition to the usual P -wave ϕ resonance in the angular analysis, the fraction of which is fitted in later analyses. The $D\bar{O}$ Collaboration finds^{153, 203–206} $\Delta\Gamma_s = 0.163^{+0.065}_{-0.064} \text{ ps}^{-1}$ and $\tau(B_s^0) = 1/\Gamma_s = 1.443 \pm 0.038 \text{ ps}$, while CDF measures^{164, 207–210} $\Delta\Gamma_s = 0.068 \pm 0.026 \text{ (stat)} \pm 0.007 \text{ (syst)} \text{ ps}^{-1}$ and $\tau(B_s^0) = 1/\Gamma_s = 1.528 \pm 0.019 \text{ (stat)} \pm 0.009 \text{ (syst)} \text{ ps}$. These can be compared with the theory prediction²¹¹ of $\Delta\Gamma_s = 0.087 \pm 0.021 \text{ ps}^{-1}$ for the most stringent test of the validity of HQE.

8. CP Violation

One of the most prominent questions in particle physics is the source of the baryon-antibaryon asymmetry observed in the universe. One of the requirements for this asymmetry is CP violation. The SM naturally includes CP violation (CPV) in the quark sector through the presence of a single complex phase in the CKM matrix, which in turn determines the strength of flavor transitions through the weak interaction. However, the degree of CPV from this SM source is insufficient to explain the cosmological matter dominance.²¹² Heavy flavor systems are ideal to search for new phases and levels of CPV that depart from SM predictions. There are three kinds of CP violation, all explored at the Tevatron: direct CP violation where the probability for a particle to decay to a given final state differs from the probability for the antiparticle to decay to the charge conjugate state $|\mathcal{A}_f|^2 \neq |\bar{\mathcal{A}}_{\bar{f}}|^2$, CP violation in mixing where $|q/p| \neq 1$ (see Eq. 3), and in the interference of decay and mixing amplitudes.^b

The advantage of carrying out CPV tests at the Tevatron is the $p\bar{p}$ CP -invariant initial state, in contrast to the pp collisions at the LHC, where production asymmetries need to be taken into account. In the case of the DØ detector,⁴ the polarities of the toroidal and solenoidal magnetic fields were reversed on average every two weeks so that the four solenoid-toroid polarity combinations are exposed to approximately the same integrated luminosity. This allows for a cancellation of first-order effects related to instrumental charge asymmetries, particularly for tracking, to achieve levels of precision that would be difficult to reach otherwise.

8.1. CP violation in charm

CDF has studied CP violation in D^0 decays using the soft pion from $D^{*\pm}$ decays to tag the D -meson flavor at the time of production as in the mixing measurement. Also similar to the mixing measurement, the component related to D^0 mesons produced in bottom decays is subtracted using the D^0 impact parameter information. Following initial studies²¹³ with small data samples, CDF searched²¹⁴ in a 5.9 fb^{-1} sample for CP violation in the decays to CP eigenstates $D^0 \rightarrow K^+K^-$ and $D^0 \rightarrow \pi^+\pi^-$ and found results that were consistent with both the standard model and significant CP violation. The individual asymmetries from direct and indirect CP violation cannot be determined from a time-integrated measurement. The figure shows that band that is allowed based on the mean decay time of the sample.

Theoretical calculations²¹⁵ indicated that CPV in the charm system should be small, of order 10^{-3} . Thus a large difference ΔA_{CP} between the asymmetries for $\pi\pi$ and KK would indicate a large asymmetry in one mode or both. Taking the difference also has the advantage of canceling production asymmetries as well as production biases. LHCb was able to use this technique to find the first evidence²¹⁶ of CP violation in charm decays. CDF followed up²¹⁷ using the full dataset and includ-

^btest

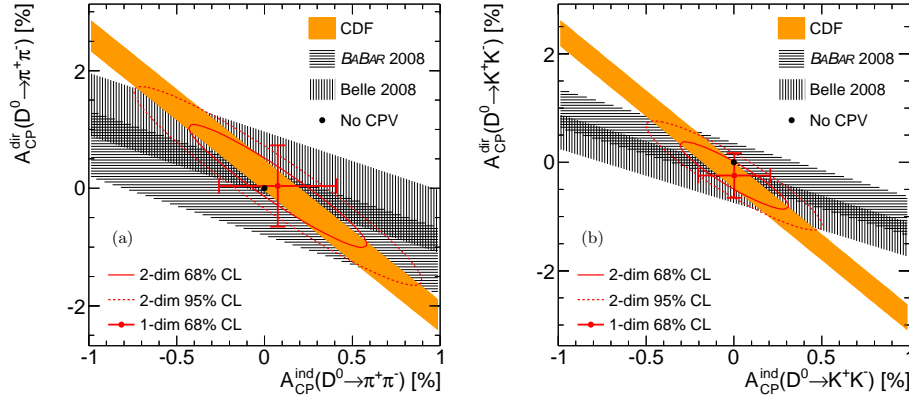


Fig. 23. (a) CDF results on CP violation in $D^0 \rightarrow \pi^+\pi^-$ decays. The asymmetries from direct and indirect CP violation. The allowed band is a function of the mean decay time of the sample. (b) Results for $D^0 \rightarrow K^+K^-$ decays.

ing events with a looser selection than the original analysis. The three observables were the $\pi\pi$ asymmetry and KK asymmetry using the original selections as well as the difference in asymmetries from the subsample with the looser selection. The new result improved the individual asymmetry measurements and confirmed the LHCb measurement of a difference from zero in ΔA_{CP} at nearly the 3σ level. The CDF measurements of the individual asymmetries are the most precise in the world.

CDF has also searched²¹⁸ for CPV in $D^0 \rightarrow K_S^0\pi^+\pi^-$ decays. Two complementary approaches are used: a full Dalitz fit employing the isobar model for the involved resonances and a model-independent bin-by-bin comparison of the D^0 and \bar{D}^0 Dalitz plots. No evidence of CP violation is found.

The DØ Collaboration has searched for direct CPV in charm decay. Since all of the contributing processes to each of the decays $D_s^\pm \rightarrow \phi\pi^\pm$ and $D^\pm \rightarrow K^\mp\pi^\pm$ have the same weak phase in each case, there should be no direct CPV for these channels, so that any non-zero value could point towards new physics. The CP asymmetry of these channels is also assumed to be zero for a number of other heavy flavor CP measurements. DØ has made the most precise measurements^{219, 220} of these CP asymmetries, and they are indeed consistent with zero.

8.2. Direct CP violation in B decays

Two-body charmless hadronic decays of b hadrons are an important avenue for the study of direct CP violation. While CP asymmetries of B^0 and B^+ mesons can be studied at e^+e^- colliders, a complete understanding can be achieved only by comparing results to those for B_s^0 meson which are the exclusive domain of hadron colliders. The study of charmless modes of Λ_b^0 also offers the opportunity to search for physics beyond the standard model. The CDF SVT was designed for the purpose

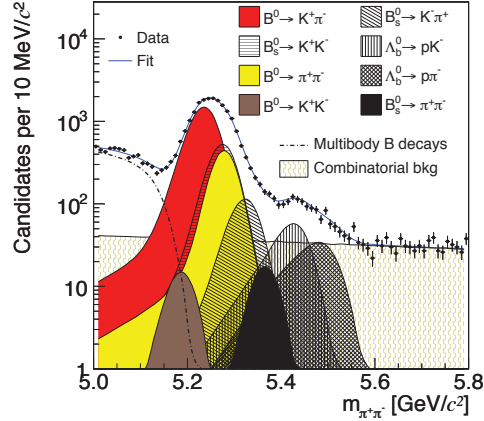


Fig. 24. Mass distribution of reconstructed candidates in two-body charmless decays where the charged pion mass is assigned to both tracks in the full 9.6 fb^{-1} sample from CDF. The sum of the fitted distributions and the individual components (conjugate decay modes are also implied) of signal and background are overlaid on the data distribution. The degeneracy of the different components is broken using particle identification and kinematic information.

of identifying two-body charmless decays in the trigger.²²¹

With a sample of only 180 pb^{-1} , CDF was able to make the first observation²²² of a charmless B_s^0 decay mode. While the signature of a two-particle decay that is displaced from the beamline gives a quite clean signal for decays of the form $B_{(s)} \rightarrow h^+ h'^-$ where h and h' are either pions or kaons, the signals from the various modes are nearly degenerate in mass. Therefore, it is necessary to use particle identification coupled with kinematic information to disentangle the various modes. While measurements of dE/dx in the CDF drift chamber cannot provide event-by-event identification, when included in a likelihood fit along with the mass and the asymmetry between the h^+ and h'^- momenta, the yields in the various modes can be determined. Thus CDF was able to observe $B_s^0 \rightarrow K^+ K^-$ and to make measurements of the branching ratios of $B^0 \rightarrow \pi^+ K^-$ and $B^0 \rightarrow \pi^+ \pi^-$ that were nearly as good as those from B factories at that time.²²³

Using similar methods, in a sample of 1 fb^{-1} CDF was made the first observation²²⁴ of the decay modes $B_s^0 \rightarrow K^- \pi^+$, $\Lambda_b^0 \rightarrow p K^-$, and $\Lambda_b^0 \rightarrow p \pi^-$, each with greater than 6σ significance, and measured their branching ratios. Differences between CP asymmetries in $B^0 \rightarrow K^+ \pi^-$ and $B^+ \rightarrow K^+ \pi^0$ observed at the b factories^{225–227} is significantly larger than naive expectations of the SM.^{228, 229} Insight into theoretical explanations of these results can be found from the asymmetry in $B_s^0 \rightarrow K^- \pi^+$ decays. Using improved techniques in the 1 fb^{-1} sample, CDF made the first measurement²³⁰ of this quantity as well as improved measurements of the branching ratios of $B^0 \rightarrow \pi^+ \pi^-$ and $B_s^0 \rightarrow K^+ K^-$ and the first measurements of asymmetries in $\Lambda_b^0 \rightarrow p K^-$, and $\Lambda_b^0 \rightarrow p \pi^-$ decays. Further progress in B_s^0

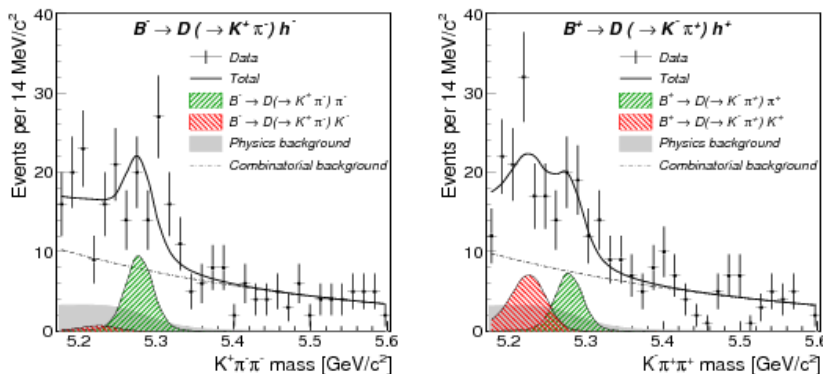


Fig. 25. Invariant mass distributions of the suppressed mode $B^\pm \rightarrow D^0 h^\pm$. The pion mass is assigned to the charged track from the B candidate decay vertex.

decays came with 6.1fb^{-1} and the first evidence²³¹ for the charmless annihilation decay mode $B_s^0 \rightarrow \pi^+\pi^-$. Subsequently, LHCb made the first observation²³² of CP violation in B_s^0 decays. Using the full 9.6fb^{-1} dataset, CDF confirmed²³³ that observation. The asymmetry measurements in the charmless Λ_b^0 decay modes have better than 10% precision and show no significant asymmetry. Those measurements remain unique to CDF.

In the 180pb^{-1} sample, CDF also searched²³⁴ for CP violation in $B^+ \rightarrow \phi K^+$ decays. The asymmetry was consistent with zero, but the measurement was competitive with those from Belle²³⁵ and Babar.²³⁶

The SM predicts that for $b \rightarrow c\bar{c}s$ decays, the tree and penguin contributions have the same weak phase, and thus no direct CP violation is expected in $B^+ \rightarrow J/\psi K^\pm$ decays, although there may be a tiny amount due to penguin loops. The DØ Collaboration has made the best precision measurement^{237, 238} of the CP asymmetry between the width of $B^+ \rightarrow J/\psi K^+$ and its charge conjugate and finds that is consistent with zero.

Taking advantage of the displaced-track trigger, CDF has also studied CP violation in hadronic decay modes with $b \rightarrow c$ transitions. The branching fractions and CP asymmetries of $B^\pm \rightarrow D^0 h^\pm$ modes, where h is a pion or kaon, allow a theoretically-clean way of measuring the CKM angle γ which is the least well-known CKM angle.¹⁰⁰ The ADS method^{239, 240} takes advantage of the the large interference between the process in which a $B^- \rightarrow D^0 h^-$ decay through a color-allowed $b \rightarrow c$ transition is followed by the doubly Cabibbo-suppressed $D^0 \rightarrow K^+\pi^-$ decay and the process in which a $B^- \rightarrow \bar{D}^0 h^-$ decay through a color-suppressed $b \rightarrow u$ transition followed by the Cabibbo-favored decay $\bar{D}^0 \rightarrow K^+\pi^-$. This interference can lead to significant CP asymmetries from which γ can be extracted. CDF observed^{241, 242} both the $B^- \rightarrow [K^+\pi^-]_D K^-$ and $B^- \rightarrow [K^+\pi^-]_D \pi^-$ modes with

greater than 3σ significance and measured the rates and asymmetries.

8.3. *CP violation in B mixing*

CP violation can develop in the mixing of the neutral B meson system if the 2×2 mass and decay matrix described in Sect. 7 has a non-zero phase $\phi = \arg[-M_{12}/\Gamma_{12}]$ between the off-diagonal elements that are responsible for the mixing. The time-integrated flavor-specific semileptonic charge asymmetry is defined as

$$a_{\text{sl}}^{d(s)} = \frac{\Gamma(\bar{B}_{(s)}^0 \rightarrow B_{(s)}^0 \rightarrow \ell^+ X) - \Gamma(B_{(s)}^0 \rightarrow \bar{B}_{(s)}^0 \rightarrow \ell^- X)}{\Gamma(\bar{B}_{(s)}^0 \rightarrow B_{(s)}^0 \rightarrow \ell^+ X) + \Gamma(B_{(s)}^0 \rightarrow \bar{B}_{(s)}^0 \rightarrow \ell^- X)} = \frac{\Delta\Gamma_q}{\Delta m_q} \tan \phi_q \quad (7)$$

that is also equivalent to $(|p/q|^2 - |q/p|^2)/(|p/q|^2 + |q/p|^2)$.

By measuring the asymmetry between the number of reconstructed $B^0 \rightarrow D^{(*)-}\mu^+X$ decays compared to the charge conjugate $D^{(*)+}\mu^-$ in bins of visible proper decay length and then correcting for detector asymmetries as shown in Fig. 26(a), the DØ Collaboration measured²⁴³ $a_{\text{sl}}^d = [0.68 \pm 0.45 (\text{stat.}) \pm 0.14 (\text{syst.})]\%$, which is the single most precise measurement of this parameter, with uncertainties smaller than the previous world average of B factory measurements, and consistent with the SM prediction²¹¹ of $< 10^{-3}$. The DØ Collaboration performed a similar analysis using time-integrated $B_s^0 \rightarrow D_s^- \mu^+ X$ fitting simultaneously to the sum and the difference of the two charge-conjugate processes as shown in Fig. 26(b,c) to measure^{244,245} $a_{\text{sl}}^s = [1.12 \pm 0.74 (\text{stat}) \pm 0.17 (\text{syst})]\%$, the most precise measurement at the time, consistent with the current LHCb measurement²⁴⁶ and small value of the SM prediction.²¹¹

One of the few ways for direct physics (*i.e.* excluding pion and kaon decays in flight) to result in a pair of same-sign muons is when a b hadron directly decays semileptonically, while a neutral B meson from the other produced b quark oscillates before decaying semileptonically. *CP* violation in mixing can be expressed as $\Gamma(B_{(s)}^0 \rightarrow \bar{B}_{(s)}^0 \rightarrow \mu^- X) \neq \Gamma(\bar{B}_{(s)}^0 \rightarrow B_{(s)}^0 \rightarrow \mu^- X)$ and can be explored by studying the semileptonic asymmetry $\mathcal{A}_{\text{sl}}^b = [N_b(\mu^+\mu^+) - N_b(\mu^-\mu^-)]/\text{sum}$ by forming the raw asymmetry, correcting for background asymmetries using independent data samples, and determining the fraction of muons from b quarks. This asymmetry is a linear combination of the semileptonic charge asymmetries of B^0 and B_s^0 , *i.e.* $\mathcal{A}^b = C_d a_{\text{sl}}^d + C_s a_{\text{sl}}^s$.

In previous publications,^{247–250} the DØ Collaboration measured \mathcal{A}^b with increasingly larger datasets with values representing up to a 3.9σ deviation from the SM prediction. The analysis¹⁹³ with the full Run 2 dataset added a more detailed study of the asymmetry dependence on the impact parameter (IP), p_T , and $|\eta|$ of each muon, as well as including an additional *CP*-violating process to interpret results.²⁵¹ Measurements in the dimuon sample shown in Fig. 27(a) give a result of A_{CP} that represents a 3.6σ deviation from the SM prediction which is the largest observed deviation in the heavy flavor physics program at the Tevatron. Since the fractional mix of B^0 and B_s^0 is different in each (IP₁, IP₂) bin, the semileptonic charge asym-

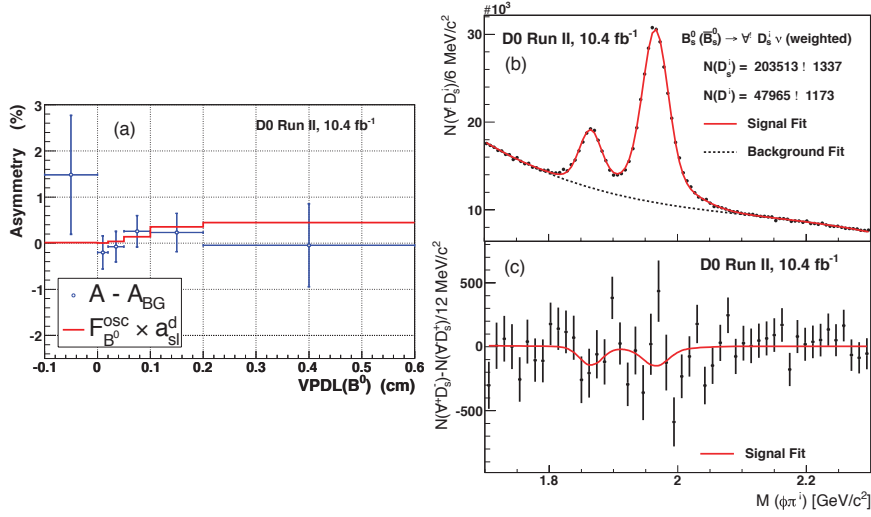


Fig. 26. (a) Background-corrected semileptonic charge asymmetry versus visible proper decay length of B^0 . (b) Sum of B_s^0 (\bar{B}_s^0) $\rightarrow D_s^\mp \mu^\pm$; and (c) difference between the two conjugate states.

metries can be extracted as shown in Fig. 27(b). The result deviates from the SM by 3.0σ . The results are consistent with the independent $D\bar{D}$ measurements^{243,244} of a_{sl}^d and a_{sl}^s described above, and the combination of all $D\bar{D}$ results are also shown in Fig. 27(b). These are the most precise determinations of these quantities so far from a single measurement. The observed dimuon charge asymmetry also has a contribution from the CP violation in the interference of decay amplitudes for the decay $B^0(\bar{B}^0) \rightarrow c\bar{c}d\bar{d}$ with and without mixing.²⁵¹ Since this contribution is proportional to the quantity $\Delta\Gamma_d/\Gamma_d$, the measurement also allows for the extraction of $\Delta\Gamma_d/\Gamma_d = (0.50 \pm 1.38)\%$ (and $(0.79 \pm 1.15)\%$ when combining all the $D\bar{D}$ measurements). This combination is still consistent with all other measurements, and also stresses the importance of having more independent measurements of $\Delta\Gamma_d/\Gamma_d$.

8.4. CP violation in interference between decay and B mixing

In the “golden mode” of the B factories, the final state of $J/\psi K^0$ can be reached directly from B^0 decay or after a flavor oscillation, *i.e.* $B^0 (\rightarrow \bar{B}^0) \rightarrow J/\psi K^0$. There is interference since the same final state can be reached by two different decay paths, and CPV can occur in this interference via phases ϕ^{NP} arising from new physics. This decay explores the unitarity triangle formed from the first and third columns of the CKM matrix and can be used to measure precisely the angle β . The corresponding golden modes at the Tevatron are decays of the type $B_s^0 (\rightarrow \bar{B}_s^0) \rightarrow J/\psi \phi$ that probe the “squashed” unitarity triangle for the B_s^0 system formed from the second and third columns of the CKM matrix characterized by the tiny angle²¹¹ $\beta_s^{\text{SM}} = \arg[-V_{ts}V_{tb}^*/V_{cs}V_{cb}^*] \simeq 0.02$. In the absence of new physics, the CPV

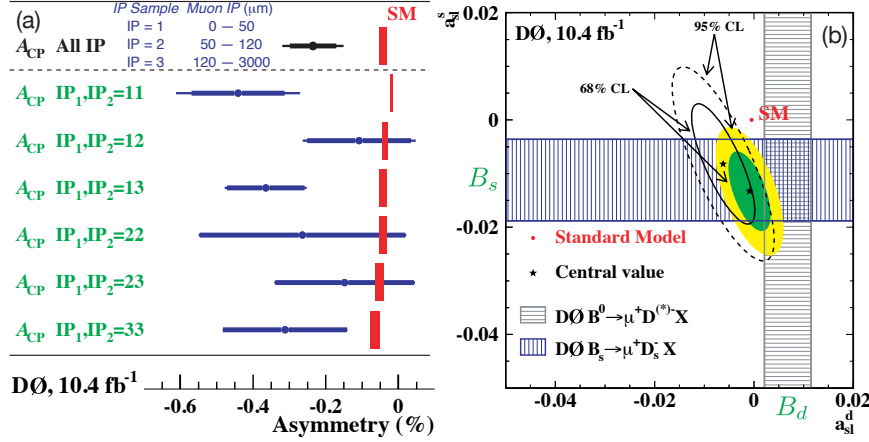


Fig. 27. (a) Dimuon charge CP asymmetry A_{CP} in bins of impact parameter (IP) of each of the two muons and over entire sample. (b) Result (black dashed and solid line contours) of dimuon charge asymmetry as a function of semileptonic CP charge asymmetry a_{sl}^s and a_{sl}^d . Solid colored contours after combination with independent direct measurements (hashed bands) from D^0 .

phase measured in these analyses will give $\phi_s = 2\beta_s^{SM}$, too small to resolve with the sensitivities of the Tevatron experiments, while giving $\phi_s = 2\beta_s^{SM} + \phi^{NP}$ in the presence of new phases that potentially could be observed.

CP violation can therefore be manifested in a difference between the decays $B_s^0 (\rightarrow \bar{B}_s^0) \rightarrow J/\psi \phi$ and $\bar{B}_s^0 (\rightarrow B_s^0) \rightarrow J/\psi \phi$. The angular distributions of the decays of the two vector particles in the final state $J/\psi \rightarrow \mu^+ \mu^-$ and $\phi \rightarrow K^+ K^-$ can be used to disentangle the CP -even and CP -odd components as a function of proper decay time. With a sizable lifetime difference $\Delta\Gamma_s$, there is sensitivity to ϕ_s through the interference terms between the CP -even and CP -odd states even without flavor-tagging the initial state. In the approach pursued in early analyses by D^0 ^{205,206} and CDF,²⁰⁷ the lifetime difference $\Delta\Gamma_s$, average lifetime $\bar{\tau}_s = 1/\Gamma_s$, and ϕ_s were measured. These early analyses generated considerable excitement as both Tevatron experiments indicated modest deviations from the SM, both to negative values as shown in Fig. 28 that when combined²⁵² gave a 2.2σ deviation from the SM, and 2.7σ when combined with the value of a_{sl}^s at that time, as shown in Fig. 28(a). Later analyses^{203,204,209,210} included initial-state flavor tagging as well as taking into account any S -wave $K^+ K^-$ component under the ϕ mass peak. Final analyses give results consistent with both later measurements at LHC and with the SM (see Fig. 28(b)).

In the 180 pb^{-1} sample, CDF made the first observation²³⁴ of a charmless B_s^0 decay, measuring the branching ratio of $B_s^0 \rightarrow \phi\phi$. Because there are two vector particles in the final state, the angular distributions for this decay mode can be expressed in terms of three complex amplitudes. The full description includes the

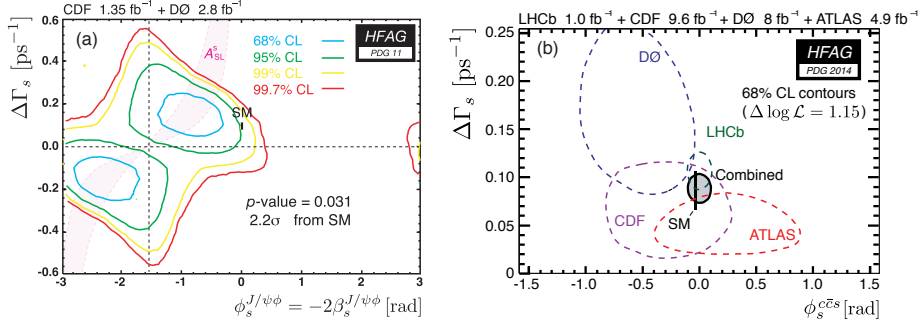


Fig. 28. (a) Combined CDF and $D\bar{0}$ constraints on the B_s^0 lifetime difference $\Delta\Gamma_s$ and CP -violating phase ϕ_s for PDG 2011; and (b) individual final constraints compared to and combined with results from LHC experiments.

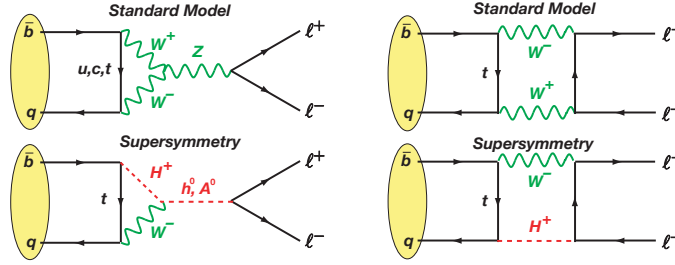


Fig. 29. In the SM, FCNC decays can proceed through box and loop W and Z diagrams, while in SM extensions new particles can contribute to the processes and increase the branching fractions.

time evolution of the heavy and light CP eigenstates of the B_s^0 . The general expression for the angular distributions contains terms whose coefficients are zero in the SM, thus providing another avenue to search for new physics. CDF has measured²⁵³ the amplitudes of the angular distributions and searched for asymmetries in components sensitive to new physics. No significant asymmetries were found. The branching ratio is $\text{BR}(B_s^0 \rightarrow \phi\phi) = [2.32 \pm 0.18 (\text{stat}) \pm 0.82 (\text{syst})] \times 10^{-5}$. The longitudinal fraction of decays can be used to understand the details of the decay process and is found to be $f_L = 0.348 \pm 0.041(\text{stat}) \pm 0.021(\text{syst})$.

9. Rare Decays

Flavor-changing neutral current (FCNC) decay modes are forbidden at the tree level in the SM by the GIM mechanism. They can proceed through higher-order effective FCNC currents as shown in Fig. 29. While highly suppressed in the SM, many extensions to the SM allow for the branching fractions to be increased, which makes these decays highly sensitive probes for physics beyond the SM.

9.1. FCNC decays of charm

The GIM suppression in D meson decays is significantly stronger than for B mesons because of the smaller quark masses, and the SM branching fractions are expected to be lower, leaving a large window of opportunity still available to search for new physics in charm decays. CDF searched²⁵⁴ for the decay $D^0 \rightarrow \mu^+\mu^-$ and set an upper limit on the branching fraction 3.0×10^{-7} at the 95% confidence level using the kinematically similar $D^0 \rightarrow \pi^+\pi^-$ channel for normalization. The DØ Collaboration made the first observation of the decay $D_s^+ \rightarrow \phi\pi^+ \rightarrow \mu^+\mu^-\pi^+$ and the first evidence for the decay D^+ to the same final state.²⁵⁵ The search for the $c \rightarrow u\mu^+\mu^-$ transition in the decay $D^+ \rightarrow \mu^+\mu^-\pi^+$ was performed in the continuum region outside of the ϕ resonance to set a limit of $\mathcal{B}(D^+ \rightarrow \pi^+\mu^+\mu^-) < 3.9 \times 10^{-6}$ at the 90% C.L., the most stringent on this transition at the time.

9.2. FCNC decays of b hadrons

In B mesons, internal quark annihilation decays are suppressed by $(f_B/m_B)^2 \simeq 2 \times 10^{-3}$ relative to the electroweak penguin $b \rightarrow s\gamma$ decay. Helicity suppression factor factors then push the SM branching fractions for $\mathcal{B}(B_s^0 \rightarrow \mu^+\mu^-)$ and $\mathcal{B}(B^0 \rightarrow \mu^+\mu^-)$ down to $(3.2 \pm 0.3) \times 10^{-9}$ and $(1.1 \pm 0.1) \times 10^{-10}$, respectively.²⁵⁶

Aside from a weak constraint²⁵⁷ from the L3 Collaboration at LEP, the Tevatron experiments provided the only significant bounds on $\mathcal{B}(B_q^0 \rightarrow \mu^+\mu^-)$ for decades, contributing strongly to placing powerful constraints on BSM physics. As an example, the decay rate for $B_s^0 \rightarrow \mu^+\mu^-$ is proportional to $(\tan\beta)^6$ in the minimal supersymmetric standard model and to $(\tan\beta)^4$ in more generic two-Higgs doublet models, where $\tan\beta$ is the ratio of the vacuum expectation values of the two Higgs fields, so that decay rate can be enhanced relative to the SM by over two orders of magnitude at large $\tan\beta$ values. An overview of these constraints on various models as well as a model-independent treatment can be found in Ref. 258.

The CDF and DØ Collaborations carried out a series of increasingly sophisticated searches for $B_s^0 \rightarrow \mu^+\mu^-$ over time as more data became available. The analyses focused on reduction of combinatorial and physics background through B_s^0 lifetime significance, muon isolation, and other kinematic criteria. CDF's first Run 2 result²⁵⁹ yielded a branching ratio 95% CL upper limit of 6×10^{-7} . This was quickly surpassed by the first Run 2 DØ analysis.²⁶⁰ Subsequent analyses by both experiments used multivariate analyses and more data with the two experiments achieving similar sensitivities as a result of their relative strengths, CDF's tracking resolution versus DØ's greater muon acceptance. The later DØ analyses used a likelihood ratio selection,²⁶¹ Bayesian neural nets,²⁶² and finally, with the full data set²⁶³ two separate boosted decision trees treating different categories of physics backgrounds, resulting in the limit $\mathcal{B}(B_s^0 \rightarrow \mu^+\mu^-) < 1.5 \times 10^{-8}$ at the 95% C.L. as shown in Fig. 30(b) and Fig. 31. Since the DØ detector did not have the necessary mass resolution to separate B^0 from B_s^0 decays, it was assumed that there are no contributions from $B^0 \rightarrow \mu^+\mu^-$ decays, since this decay is suppressed by $|V_{td}/V_{ts}|^2 \simeq 0.04$. Multi-

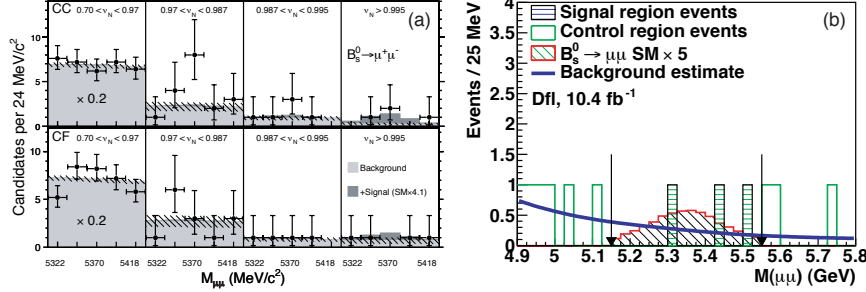


Fig. 30. (a) Results of CDF search for $B_s^0 \rightarrow \mu^+ \mu^-$ showing the dimuon mass distribution for four bins of neural net score and two sets of muon detectors. The light shaded region is the predicted background with the hatching showing its uncertainty, the points show the data, and the dark shading is the best fit for the signal. (b) D0 dimuon mass distribution in the blinded region for the full dataset after BDT selections are applied.

variate techniques substantially improved CDF's sensitivity where using a likelihood technique improved the limit²⁶⁴ by a factor of 4 after only doubling the integrated luminosity. In the analysis²⁶⁵ of 2 fb^{-1} , CDF improved the muon selection and applied a neural net classifier. The limit was calculated using several bins of neural net score with different background suppression factors in order to improve sensitivity. In a 7 fb^{-1} sample, CDF found²⁶⁶ a small excess above expected backgrounds that was more consistent with SM production than with the null hypothesis, but not sufficiently significant to claim discovery. Backgrounds in this study were verified in comparisons to data in orthogonal samples. This result was confirmed in the full dataset, leading to the result²⁶⁷ $\mathcal{B}(B_s^0 \rightarrow \mu^+ \mu^-) = (1.3_{-0.7}^{+0.9}) \times 10^{-8}$.

To explore the quark-level transition $b \rightarrow s \ell^+ \ell^-$, inclusive FCNC decays like $B^0 \rightarrow X_s \ell^+ \ell^-$ or $B^0 \rightarrow X_s \gamma$ are theoretically easier to calculate, but exclusive decays such as $B^0 \rightarrow K^* \ell^+ \ell^-$ with one hadron in the final state are experimentally easier to study at the B factories. The analogous state $B_s^0 \rightarrow \phi \ell^+ \ell^-$ tests the same transition and has been explored at the Tevatron. The D0 Collaboration searched²⁶⁸ for the decay $B_s^0 \rightarrow \phi \mu^+ \mu^-$, restricting the invariant mass of the dimuons to be outside the charmonium resonances to avoid large interference effects with dominant decay modes such as $B_s^0 \rightarrow J/\psi \phi$, and set a limit that was the most stringent at the time.

CDF made the first observation²⁶⁹ of $b \rightarrow s \mu^+ \mu^-$ decays at a hadron collider in a sample of about 1 fb^{-1} and measured branching ratios for the $B^+ \rightarrow K^+ \mu^+ \mu^-$, $B^0 \rightarrow K_S^0 \mu^+ \mu^-$, and $B^0 \rightarrow K^{*0} \mu^+ \mu^-$ decay modes. With a factor of four increase in data, CDF made the first observation²⁷⁰ of the decay $B_s^0 \rightarrow \phi \mu^+ \mu^-$ and measured the differential decay rate $d\Gamma/dq^2$ and the dimuon forward-backward asymmetry A_{FB} as a function of $q^2 \equiv M^2(\mu^+ \mu^-)$ in $B^+ \rightarrow K^+ \mu^+ \mu^-$ and $B^0 \rightarrow K^{*0} \mu^+ \mu^-$ decays as well as the longitudinal polarization fraction F_L as a function of q^2 in the B^0 mode. Because the presence of new particles mediating these FCNC

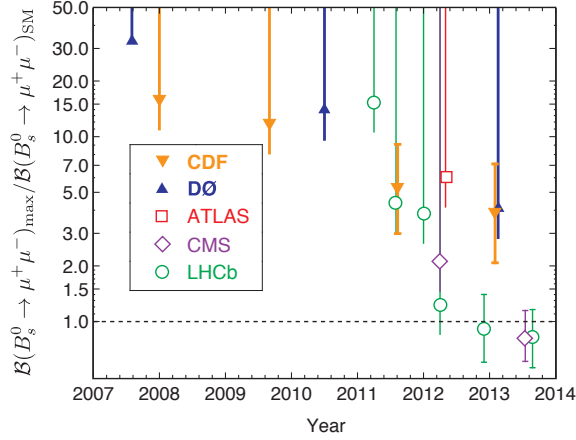


Fig. 31. History of $\mathcal{B}(B_s^0 \rightarrow \mu^+\mu^-)$ results. Symbols with one-sided bars represent 95% C.L. limits, and symbols with two-sided error bars indicate measurements.

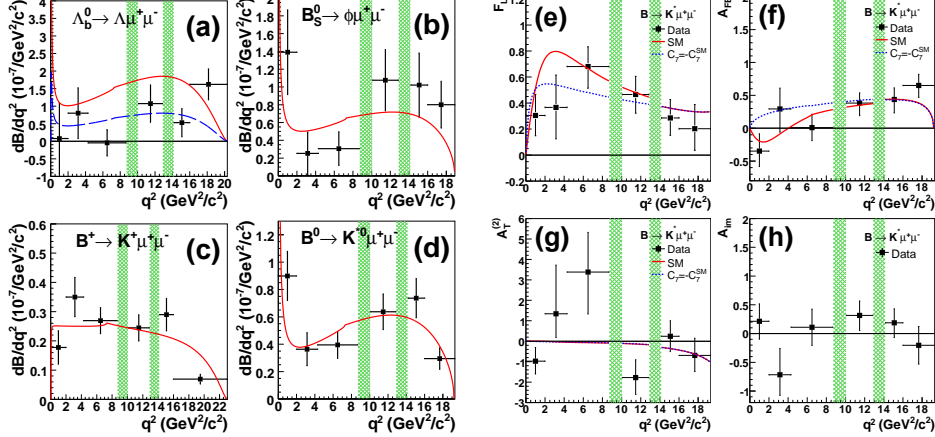


Fig. 32. Distributions as a function of q^2 for various FCNC decays measured by CDF. Differential branching ratios for (a) $\Lambda_b^0 \rightarrow \Lambda \mu^+ \mu^-$, (b) $B_s^0 \rightarrow \phi \mu^+ \mu^-$ (c) $B^+ \rightarrow K^+ \mu^+ \mu^-$, and (d) $B^0 \rightarrow K^{*0} \mu^+ \mu^-$ decays show good agreement with the standard model. Kinematic distributions in $B^0 \rightarrow K^{*0} \mu^+ \mu^-$ decays (e) F_L , (f) A_{FB} , (g) $A_T^{(2)}$, and (h) A_{im} are also consistent with the SM.

decays can change the internal dynamics of the decay, distributions of quantities like $d\Gamma/dq^2$, A_{FB} , and F_L provide important opportunities to search for the effects of new physics. The CDF measurements were quite competitive with those from the $e^+e^- B$ factories.^{271,272}

With improved analysis methods, in a sample of 6.8 fb^{-1} , CDF made the first observation²⁷³ of a FCNC decay of a baryon for the decay $\Lambda_b \rightarrow \Lambda \mu^+ \mu^-$ with a significance corresponding to 5.8σ . CDF also improved on branching ratios for the

meson decay modes and made the first measurement of $d\Gamma/dq^2$ in $B_s^0 \rightarrow \phi\mu^+\mu^-$ decays. Subsequently, CDF improved²⁷⁴ the measurements of A_{FB} and F_L and made the first measurements of transverse polarization asymmetry $A_T^{(2)}$ and the time-reversal-odd charge-and-parity asymmetry A_{im} , including $B^+ \rightarrow K^{*+}\mu^+\mu^-$ decays as well. Figure 32 shows various distributions from this analysis.

9.3. Lepton flavor violating decays

While neutrino oscillations show that lepton number is violated, the neutrino mass is too small for mixing to have an effect in hadron decays. Nevertheless, new particles in loops could lead to substantial deviations from SM expectations. For example, in the Pati-Salam model,²⁷⁵ leptoquarks carry quantum numbers of both quarks and leptons. CDF searched²⁷⁶ for the lepton-flavor violating decay $B_{s,d}^0 \rightarrow e^\pm\mu^\mp$ and set what was then the most stringent limit on the branching ratios. Those limits correspond to a 90% CL lower limit on leptoquark masses in the Pati-Salam model of 47.8 GeV (59.3 GeV) for the B^0 (B_s^0) decay mode.

10. Summary

When planning began for the Tevatron, the bottom quark had only recently been discovered. The measurement of b quark cross sections and full reconstruction of a handful B meson decays in the early data were already an achievement. While conventional wisdom held that b physics could not be done in the busy hadron collision environment, early in Run 1, CDF and DØ were breaking new ground and making world-leading measurements, often surprising their LEP competitors at the time with their capabilities. The improvements in technology and increases in luminosity that came with Run 2 coupled with the ingenuity of analyzers led to an explosion of heavy flavor results including the discovery of B_s mixing and new baryons, world-leading measurements of CP violation and b hadron properties, and precision results on heavy-quark and quarkonium production and spectroscopy.

Acknowledgments

We thank Marjorie Corcoran, Mark Williams, and Daria Zieminska for reviewing and providing valuable comments. We also thank the Fermilab staff and technical staffs of the participating institutions for their vital contributions. We acknowledge support from the DOE and NSF (USA), ARC (Australia), CNPq, FAPERJ, FAPESP and FUNDUNESP (Brazil), NSERC (Canada), NSC, CAS and CNSF (China), Colciencias (Colombia), MSMT and GACR (Czech Republic), the Academy of Finland, CEA and CNRS/IN2P3 (France), BMBF and DFG (Germany), DAE and DST (India), SFI (Ireland), INFN (Italy), MEXT (Japan), the KoreanWorld Class University Program and NRF (Korea), CONACyT (Mexico), FOM (Netherlands), MON, NRC KI and RFBR (Russia), the Slovak R&D Agency, the Ministerio de Ciencia e Innovacion, and Programa Consolider–Ingenio 2010

(Spain), The Swedish Research Council (Sweden), SNSF (Switzerland), STFC and the Royal Society (United Kingdom), the A.P. Sloan Foundation (USA), and the EU community Marie Curie Fellowship contract 302103.

References

1. V. Abazov *et al.*, *Nucl. Instrum. Meth.* **A552**, 372 (2005),
[arXiv:physics/0503151](#) [[physics.ins-det](#)].
2. A. Bardi, A. Belloni, R. Carosi, G. Chlachidze, M. Dell’Orso *et al.*, *Nucl. Instrum. Meth.* **A485**, 178 (2002).
3. CDF Collaboration (A. A. Affolder *et al.*), *Nucl. Instrum. Meth.* **A526**, 249 (2004).
4. DØ Collaboration (V. Abazov *et al.*), *Nucl. Instrum. Meth.* **A565**, 463 (2006),
[arXiv:physics/0507191](#) [[physics.ins-det](#)].
5. CDF Collaboration (T. Aaltonen *et al.*), *Nucl. Instrum. Meth.* **A729**, 153 (2013),
[arXiv:1301.3180](#) [[physics.ins-det](#)].
6. S. Ahmed *et al.*, *Nucl. Instrum. Meth.* **A634**, 8 (2011),
[arXiv:1005.0801](#) [[physics.ins-det](#)].
7. R. Angstadt *et al.*, *Nucl. Instrum. Meth.* **A622**, 298 (2010),
[arXiv:0911.2522](#) [[physics.ins-det](#)].
8. CDF Collaboration (D. Acosta *et al.*), *Nucl. Instrum. Meth.* **A518**, 605 (2004).
9. UA1 Collaboration (C. Albajar *et al.*), *Phys. Lett. B* **186**, 237 (1987).
10. UA1 Collaboration (C. Albajar *et al.*), *Phys. Lett. B* **213**, 405 (1988).
11. UA1 Collaboration (C. Albajar *et al.*), *Phys. Lett. B* **256**, 121 (1991).
12. CDF Collaboration (F. Abe *et al.*), *Phys. Rev. Lett.* **71**, 500 (1993).
13. CDF Collaboration (F. Abe *et al.*), *Phys. Rev. Lett.* **71**, 2396 (1993).
14. CDF Collaboration (F. Abe *et al.*), *Phys. Rev. Lett.* **69**, 3704 (1992).
15. UA1 Collaboration (G. Arnison *et al.*), *Phys. Lett. B* **147**, 222 (1984).
16. CDF Collaboration (F. Abe *et al.*), *Phys. Rev. Lett.* **64**, 348 (1990).
17. CDF Collaboration (F. Abe *et al.*), *Phys. Rev. Lett.* **68**, 3403 (1992).
18. CDF Collaboration (F. Abe *et al.*), *Phys. Rev. Lett.* **67**, 3351 (1991).
19. C. H. Haber, W. C. Carithers, R. P. Ely, S. Holland, F. Kirsten *et al.*, *Nucl. Instrum. Meth.* **A289**, 388 (1990).
20. CDF Collaboration (F. Abe *et al.*), *Phys. Rev. Lett.* **71**, 3421 (1993).
21. CDF Collaboration (F. Abe *et al.*), *Phys. Rev. Lett.* **72**, 3456 (1994).
22. CDF Collaboration (F. Abe *et al.*), *Phys. Rev. Lett.* **74**, 4988 (1995),
[arXiv:hep-ex/9412017](#) [[hep-ex](#)].
23. CDF Collaboration (F. Abe *et al.*), *Phys. Rev. Lett.* **76**, 4462 (1996).
24. CDF Collaboration (F. Abe *et al.*), *Phys. Rev. Lett.* **77**, 1439 (1996).
25. CDF Collaboration (F. Abe *et al.*), *Phys. Rev. Lett.* **77**, 1945 (1996).
26. CDF Collaboration (F. Abe *et al.*), *Phys. Rev. D* **57**, 5382 (1998).
27. CDF Collaboration (F. Abe *et al.*), *Phys. Rev. D* **58**, 092002 (1998),
[arXiv:hep-ex/9806018](#) [[hep-ex](#)].
28. CDF Collaboration (F. Abe *et al.*), *Phys. Rev. D* **59**, 032004 (1999),
[arXiv:hep-ex/9808003](#) [[hep-ex](#)].
29. CDF Collaboration (D. Acosta *et al.*), *Phys. Rev. D* **65**, 092009 (2002).
30. CDF Collaboration (F. Abe *et al.*), *Phys. Rev. D* **53**, 3496 (1996).
31. CDF Collaboration (F. Abe *et al.*), *Phys. Rev. D* **55**, 1142 (1997).
32. CDF Collaboration (F. Abe *et al.*), *Phys. Rev. Lett.* **79**, 572 (1997).
33. CDF Collaboration (F. Abe *et al.*), *Phys. Rev. Lett.* **75**, 4358 (1995).
34. CDF Collaboration (T. Affolder *et al.*), *Phys. Rev. Lett.* **84**, 2094 (2000),

- arXiv:hep-ex/9910025 [hep-ex].
35. CDF Collaboration (D. Acosta *et al.*), *Phys.Rev.Lett.* **88**, 161802 (2002).
 36. CDF Collaboration (T. Affolder *et al.*), *Phys. Rev. Lett.* **85**, 2886 (2000),
arXiv:hep-ex/0004027 [hep-ex].
 37. CDF Collaboration (F. Abe *et al.*), *Phys. Rev. Lett.* **79**, 578 (1997).
 38. CDF Collaboration (T. Affolder *et al.*), *Phys. Rev. Lett.* **86**, 3963 (2001).
 39. CDF Collaboration (F. Abe *et al.*), *Phys. Rev. D* **50**, 4252 (1994).
 40. CDF Collaboration (F. Abe *et al.*), *Phys. Rev. Lett.* **75**, 1451 (1995),
arXiv:hep-ex/9503013 [hep-ex].
 41. CDF Collaboration (D. Acosta *et al.*), *Phys. Rev. D* **65**, 052005 (2002),
arXiv:hep-ph/0111359 [hep-ph].
 42. CDF Collaboration (D. Acosta *et al.*), *Phys. Rev. D* **66**, 032002 (2002),
arXiv:hep-ex/0206019 [hep-ex].
 43. CDF Collaboration (T. Affolder *et al.*), *Phys. Rev. Lett.* **84**, 1663 (2000),
arXiv:hep-ex/9909011 [hep-ex].
 44. CDF Collaboration (F. Abe *et al.*), *Phys. Rev. D* **60**, 092005 (1999).
 45. CDF Collaboration (F. Abe *et al.*), *Phys. Rev. Lett.* **76**, 4675 (1996).
 46. CDF Collaboration (F. Abe *et al.*), *Phys. Rev. Lett.* **81**, 5742 (1998).
 47. CDF Collaboration (F. Abe *et al.*), *Phys. Rev. D* **57**, 3811 (1998).
 48. CDF Collaboration (D. Acosta *et al.*), *Phys. Rev. D* **65**, 111101 (2002).
 49. CDF Collaboration (D. Acosta *et al.*), *Phys. Rev. D* **66**, 112002 (2002),
arXiv:hep-ex/0208035 [hep-ex].
 50. CDF Collaboration (F. Abe *et al.*), *Phys. Rev. Lett.* **76**, 2015 (1996).
 51. CDF Collaboration (F. Abe *et al.*), *Phys. Rev. D* **54**, 6596 (1996),
arXiv:hep-ex/9607003 [hep-ex].
 52. CDF Collaboration (F. Abe *et al.*), *Phys. Rev. Lett.* **77**, 5176 (1996).
 53. CDF Collaboration (T. Affolder *et al.*), *Phys. Rev. Lett.* **85**, 4668 (2000),
arXiv:hep-ex/0007034 [hep-ex].
 54. CDF Collaboration (T. Affolder *et al.*), *Phys. Rev. Lett.* **88**, 071801 (2002),
arXiv:hep-ex/0108022 [hep-ex].
 55. CDF Collaboration (D. Acosta *et al.*), *Phys. Rev. D* **66**, 052005 (2002).
 56. CDF Collaboration (F. Abe *et al.*), *Phys. Rev. D* **58**, 072001 (1998),
arXiv:hep-ex/9803013 [hep-ex].
 57. CDF Collaboration (F. Abe *et al.*), *Phys. Rev. Lett.* **75**, 3068 (1995).
 58. CDF Collaboration (F. Abe *et al.*), *Phys. Rev. Lett.* **81**, 2432 (1998),
arXiv:hep-ex/9805034 [hep-ex].
 59. CDF Collaboration (F. Abe *et al.*), *Phys. Rev. D* **58**, 112004 (1998),
arXiv:hep-ex/9804014 [hep-ex].
 60. CDF Collaboration (F. Abe *et al.*), *Phys. Rev. D* **59**, 032001 (1999),
arXiv:hep-ex/9806026 [hep-ex].
 61. CDF Collaboration (F. Abe *et al.*), *Phys. Rev. Lett.* **82**, 3576 (1999).
 62. CDF Collaboration (F. Abe *et al.*), *Phys. Rev. D* **60**, 072003 (1999),
arXiv:hep-ex/9903011 [hep-ex].
 63. CDF Collaboration (T. Affolder *et al.*), *Phys. Rev. D* **60**, 112004 (1999),
arXiv:hep-ex/9907053 [hep-ex].
 64. CDF Collaboration (F. Abe *et al.*), *Phys. Rev. D* **60**, 051101 (1999).
 65. CDF Collaboration (F. Abe *et al.*), *Phys. Rev. Lett.* **81**, 5513 (1998),
arXiv:hep-ex/9806025 [hep-ex].
 66. CDF Collaboration (T. Affolder *et al.*), *Phys. Rev. D* **61**, 072005 (2000),
arXiv:hep-ex/9909003 [hep-ex].

67. DØ Collaboration (S. Abachi *et al.*), *Nucl. Instrum. Meth.* **A338**, 185 (1994).
68. DØ Collaboration (S. Abachi *et al.*), *Phys. Rev. Lett.* **74**, 3548 (1995).
69. DØ Collaboration (B. Abbott *et al.*), *Phys. Rev. Lett.* **84**, 5478 (2000),
[arXiv:hep-ex/9907029](#) [[hep-ex](#)].
70. DØ Collaboration (B. Abbott *et al.*), *Phys. Lett. B* **487**, 264 (2000),
[arXiv:hep-ex/9905024](#) [[hep-ex](#)].
71. DØ Collaboration (B. Abbott *et al.*), *Phys. Rev. Lett.* **85**, 5068 (2000),
[arXiv:hep-ex/0008021](#) [[hep-ex](#)].
72. DØ Collaboration (S. Abachi *et al.*), *Phys. Lett. B* **370**, 239 (1996).
73. DØ Collaboration (B. Abbott *et al.*), *Phys. Rev. Lett.* **82**, 35 (1999),
[arXiv:hep-ex/9807029](#) [[hep-ex](#)].
74. DØ Collaboration (B. Abbott *et al.*), *Phys. Lett. B* **423**, 419 (1998),
[arXiv:hep-ex/9801027](#) [[hep-ex](#)].
75. Particle Data Group Collaboration (M. Kreps and Y. Kwon), *Chin. Phys. C* **38**,
090001 (2014), review article *Production and decay of b-flavored hadrons*.
76. CDF Collaboration (A. Abulencia *et al.*), *Phys. Rev. D* **75**, 012010 (2007),
[arXiv:hep-ex/0612015](#) [[hep-ex](#)].
77. CDF Collaboration (D. Acosta *et al.*), *Phys. Rev. D* **71**, 032001 (2005),
[arXiv:hep-ex/0412071](#) [[hep-ex](#)].
78. CDF Collaboration (T. Aaltonen *et al.*), *Phys. Rev. D* **79**, 092003 (2009),
[arXiv:0903.2403](#) [[hep-ex](#)].
79. M. Cacciari, M. Greco and P. Nason, *JHEP* **9805**, 007 (1998),
[arXiv:hep-ph/9803400](#) [[hep-ph](#)].
80. M. Cacciari, S. Frixione, M. Mangano, P. Nason and G. Ridolfi, *JHEP* **0407**, 033
(2004), [arXiv:hep-ph/0312132](#) [[hep-ph](#)].
81. CDF Collaboration (T. Aaltonen *et al.*), *Phys. Rev. D* **77**, 072004 (2008),
[arXiv:0710.1895](#) [[hep-ex](#)].
82. CDF Collaboration (D. Acosta *et al.*), *Phys. Rev. Lett.* **91**, 241804 (2003),
[arXiv:hep-ex/0307080](#) [[hep-ex](#)].
83. M. Cacciari and P. Nason, *JHEP* **0309**, 006 (2003), [arXiv:hep-ph/0306212](#)
[[hep-ph](#)].
84. N. Brambilla, S. Eidelman, B. Heltsley, R. Vogt, G. Bodwin *et al.*, *Eur. Phys. J. C*
71, 1534 (2011), [arXiv:1010.5827](#) [[hep-ph](#)].
85. DØ Collaboration (V. M. Abazov *et al.*), *Phys. Rev. D* **90**, 111101 (2014),
[arXiv:1406.2380](#) [[hep-ex](#)].
86. S. Baranov, A. Snigirev, N. Zotov, A. Szczurek and W. Schfer, *Phys. Rev. D* **87**,
034035 (2013), [arXiv:1210.1806](#) [[hep-ph](#)].
87. CDF Collaboration (T. Aaltonen *et al.*), *Phys. Rev. D* **80**, 031103 (2009),
[arXiv:0905.1982](#) [[hep-ex](#)].
88. V. Khoze, A. Martin, M. Ryskin and W. Stirling, *Eur.Phys.J.* **C39**, 163 (2005),
[arXiv:hep-ph/0410020](#) [[hep-ph](#)].
89. J. Lansberg, *Eur. Phys. J.* **C61**, 693 (2009), [arXiv:0811.4005](#) [[hep-ph](#)].
90. DØ Collaboration (V. Abazov *et al.*), *Phys. Rev. Lett.* **94**, 232001 (2005),
[arXiv:hep-ex/0502030](#) [[hep-ex](#)].
91. E. L. Berger, J.-w. Qiu and Y.-l. Wang, *Phys. Rev. D* **71**, 034007 (2005),
[arXiv:hep-ph/0404158](#) [[hep-ph](#)].
92. E. L. Berger, J.-W. Qiu and Y. Wang, *Int.J.Mod.Phys.* **A20**, 3753 (2005),
[arXiv:hep-ph/0411026](#) [[hep-ph](#)].
93. DØ Collaboration (V. Abazov *et al.*), *Phys. Rev. Lett.* **101**, 182004 (2008),
[arXiv:0804.2799](#) [[hep-ex](#)].

94. P. Faccioli, C. Lourenço and J. a. Seixas, *Phys. Rev. D* **81**, 111502 (Jun 2010).
95. CDF Collaboration (T. Aaltonen *et al.*), *Phys. Rev. Lett.* **108**, 151802 (2012), [arXiv:1112.1591 \[hep-ex\]](#).
96. E. Braaten and J. Lee, *Phys. Rev. D* **63**, 071501 (Mar 2001).
97. S. Baranov and N. Zotov, *JETP Lett.* **86**, 435 (2007), [arXiv:0707.0253 \[hep-ph\]](#).
98. DØ Collaboration (V. M. Abazov *et al.*), *Phys. Rev. D* **84**, 031102 (2011), [arXiv:1105.0690 \[hep-ex\]](#).
99. CDF Collaboration (T. Aaltonen *et al.*), *Phys. Rev. D* **77**, 072003 (2008), [arXiv:0801.4375 \[hep-ex\]](#).
100. Particle Data Group Collaboration (J. Beringer *et al.*), *Phys. Rev. D* **86**, 010001 (2012).
101. LHCb Collaboration (R. Aaij *et al.*), *Phys. Rev. D* **85**, 032008 (2012), [arXiv:1111.2357 \[hep-ex\]](#).
102. LHCb Collaboration (R. Aaij *et al.*), *JHEP* **1304**, 001 (2013), [arXiv:1301.5286 \[hep-ex\]](#).
103. HFAG Collaboration (Y. Amhis *et al.*) (2012), [arXiv:1207.1158 \[hep-ex\]](#), , updated online at <http://www.slac.stanford.edu/xorg/hfag/> by the Heavy Flavor Averaging Group.
104. A. Manohar and M. Wise, *Heavy Quark Physics* (Cambridge University Press, 2000).
105. N. Isgur and M. B. Wise, *Phys. Rev. Lett.* **66**, 1130 (1991).
106. CDF Collaboration (D. Acosta *et al.*), *Phys. Rev. Lett.* **96**, 202001 (2006), [arXiv:hep-ex/0508022 \[hep-ex\]](#).
107. CDF Collaboration (A. Abulencia *et al.*), *Phys. Rev. Lett.* **96**, 082002 (2006), [arXiv:hep-ex/0505076 \[hep-ex\]](#).
108. CDF Collaboration (T. Aaltonen *et al.*), *Phys. Rev. Lett.* **100**, 182002 (2008), [arXiv:0712.1506 \[hep-ex\]](#).
109. DØ Collaboration (V. Abazov *et al.*), *Phys. Rev. Lett.* **101**, 012001 (2008), [arXiv:0802.4258 \[hep-ex\]](#).
110. DØ Collaboration (V. Abazov *et al.*), *Phys. Rev. Lett.* **99**, 172001 (2007), [arXiv:0705.3229 \[hep-ex\]](#).
111. CDF Collaboration (T. Aaltonen *et al.*), *Phys. Rev. Lett.* **102**, 102003 (2009), [arXiv:0809.5007 \[hep-ex\]](#).
112. CDF Collaboration (T. Aaltonen *et al.*), *Phys. Rev. Lett.* **100**, 082001 (2008), [arXiv:0710.4199 \[hep-ex\]](#).
113. DØ Collaboration (V. Abazov *et al.*), *Phys. Rev. Lett.* **100**, 082002 (2008), [arXiv:0711.0319 \[hep-ex\]](#).
114. CDF Collaboration (T. A. Aaltonen *et al.*), *Phys. Rev. D* **90**, 012013 (2014), [arXiv:1309.5961 \[hep-ex\]](#).
115. CDF Collaboration (A. Abulencia *et al.*), *Phys. Rev. D* **73**, 051104 (2006), [arXiv:hep-ex/0512069 \[hep-ex\]](#).
116. DØ Collaboration (V. Abazov *et al.*), *Phys. Rev. Lett.* **95**, 171803 (2005), [arXiv:hep-ex/0507046 \[hep-ex\]](#).
117. DØ Collaboration (V. Abazov *et al.*), *Phys. Rev. Lett.* **102**, 051801 (2009), [arXiv:0712.3789 \[hep-ex\]](#).
118. BaBar Collaboration (B. Aubert *et al.*), *Phys.Rev.Lett.* **97**, 222001 (2006), [arXiv:hep-ex/0607082 \[hep-ex\]](#).
119. Belle Collaboration (J. Brodzicka *et al.*), *Phys. Rev. Lett.* **100**, 092001 (2008), [arXiv:0707.3491 \[hep-ex\]](#).
120. CDF Collaboration (T. Aaltonen *et al.*), *Phys. Rev. Lett.* **99**, 202001 (2007), [arXiv:0706.3868 \[hep-ex\]](#).

121. CDF Collaboration (T. Aaltonen *et al.*), *Phys. Rev. D* **85**, 092011 (2012), [arXiv:1112.2808 \[hep-ex\]](#).
122. DØ Collaboration (V. Abazov *et al.*), *Phys. Rev. Lett.* **99**, 052001 (2007), [arXiv:0706.1690 \[hep-ex\]](#).
123. CDF Collaboration (T. Aaltonen *et al.*), *Phys. Rev. Lett.* **99**, 052002 (2007), [arXiv:0707.0589 \[hep-ex\]](#).
124. CDF Collaboration (T. Aaltonen *et al.*), *Phys. Rev. Lett.* **107**, 102001 (2011), [arXiv:1107.4015 \[hep-ex\]](#).
125. CDF Collaboration (T. A. Aaltonen *et al.*), *Phys. Rev. D* **89**, 072014 (2014), [arXiv:1403.8126 \[hep-ex\]](#).
126. CDF Collaboration (T. Aaltonen *et al.*), *Phys. Rev. D* **80**, 072003 (2009), [arXiv:0905.3123 \[hep-ex\]](#).
127. DØ Collaboration (V. Abazov *et al.*), *Phys. Rev. Lett.* **101**, 232002 (2008), [arXiv:0808.4142 \[hep-ex\]](#).
128. LHCb Collaboration (R. Aaij *et al.*), *Phys. Rev. Lett.* **110**, 182001 (2013), [arXiv:1302.1072 \[hep-ex\]](#).
129. CDF Collaboration (T. A. Aaltonen *et al.*), *Phys. Rev. D* **88**, 071101 (2013), [arXiv:1308.1760 \[hep-ex\]](#).
130. LHCb Collaboration (R. Aaij *et al.*), *Phys. Rev. Lett.* **109**, 172003 (2012), [arXiv:1205.3452 \[hep-ex\]](#).
131. CDF Collaboration (T. Aaltonen *et al.*), *Phys. Rev. D* **84**, 012003 (2011), [arXiv:1105.5995 \[hep-ex\]](#).
132. Belle Collaboration (S. Choi *et al.*), *Phys. Rev. Lett.* **91**, 262001 (2003), [arXiv:hep-ex/0309032 \[hep-ex\]](#).
133. C. Bignamini, B. Grinstein, F. Piccinini, A. Polosa and C. Sabelli, *Phys. Rev. Lett.* **103**, 162001 (2009), [arXiv:0906.0882 \[hep-ph\]](#), and references therein.
134. L. Maiani, F. Piccinini, A. Polosa and V. Riquer, *Phys. Rev. D* **71**, 014028 (2005), [arXiv:hep-ph/0412098 \[hep-ph\]](#).
135. CDF Collaboration (D. Acosta *et al.*), *Phys. Rev. Lett.* **93**, 072001 (2004), [arXiv:hep-ex/0312021 \[hep-ex\]](#).
136. DØ Collaboration (V. Abazov *et al.*), *Phys. Rev. Lett.* **93**, 162002 (2004), [arXiv:hep-ex/0405004 \[hep-ex\]](#).
137. CDF Collaboration (T. Aaltonen *et al.*), *Phys. Rev. Lett.* **103**, 152001 (2009), [arXiv:0906.5218 \[hep-ex\]](#).
138. CDF Collaboration (A. Abulencia *et al.*), *Phys. Rev. Lett.* **98**, 132002 (2007), [arXiv:hep-ex/0612053 \[hep-ex\]](#).
139. CDF Collaboration (T. Aaltonen *et al.*), *Phys. Rev. Lett.* **102**, 242002 (2009), [arXiv:0903.2229 \[hep-ex\]](#).
140. K. Yi, *Int.J.Mod.Phys. A* **28**, 1330020 (2013), [arXiv:1308.0772 \[hep-ex\]](#), and references therein.
141. DØ Collaboration (V. M. Abazov *et al.*), *Phys. Rev. D* **89**, 012004 (2014), [arXiv:1309.6580 \[hep-ex\]](#).
142. CMS Collaboration (S. Chatrchyan *et al.*), *Phys. Lett. B* **734**, 261 (2014), [arXiv:1309.6920 \[hep-ex\]](#).
143. Belle Collaboration (C. Shen *et al.*), *Phys. Rev. D* **82**, 051504 (2010), [arXiv:1008.1774 \[hep-ex\]](#).
144. LHCb Collaboration (R. Aaij *et al.*), *Phys. Rev. D* **85**, 091103 (2012), [arXiv:1202.5087 \[hep-ex\]](#).
145. DØ Collaboration (V. M. Abazov *et al.*), *Phys. Rev. D* **86**, 031103 (2012), [arXiv:1203.6034 \[hep-ex\]](#).

146. ATLAS Collaboration (G. Aad *et al.*), *Phys. Rev. Lett.* **108**, 152001 (2012), [arXiv:1112.5154 \[hep-ex\]](#).
147. C. R. Nappi, *Phys. Rev. D* **25**, 84 (1982).
148. P. Moxhay, Y. Ng and S. Tye, *Phys. Lett. B* **158**, 170 (1985).
149. CDF Collaboration (T. Aaltonen *et al.*), *Eur.Phys.J.* **C62**, 319 (2009), [arXiv:0903.2060 \[hep-ex\]](#).
150. I. I. Bigi, N. Uraltsev and A. Vainshtein, *Phys. Lett. B* **293**, 430 (1992), [arXiv:hep-ph/9207214 \[hep-ph\]](#).
151. A. Lenz (2014), [arXiv:1405.3601 \[hep-ph\]](#), and references therein.
152. DØ Collaboration (V. Abazov *et al.*), *Phys. Rev. Lett.* **102**, 032001 (2009), [arXiv:0810.0037 \[hep-ex\]](#).
153. DØ Collaboration (V. Abazov *et al.*), *Phys. Rev. Lett.* **95**, 171801 (2005), [arXiv:hep-ex/0507084 \[hep-ex\]](#).
154. DØ Collaboration (V. M. Abazov *et al.*), *Phys. Rev. D* **85**, 112003 (2012), [arXiv:1204.2340 \[hep-ex\]](#).
155. DØ Collaboration (V. Abazov *et al.*), *Phys. Rev. Lett.* **99**, 142001 (2007), [arXiv:0704.3909 \[hep-ex\]](#).
156. DØ Collaboration (V. Abazov *et al.*), *Phys. Rev. Lett.* **94**, 102001 (2005), [arXiv:hep-ex/0410054 \[hep-ex\]](#).
157. CDF Collaboration (T. Aaltonen *et al.*), *Phys. Rev. Lett.* **106**, 121804 (2011), [arXiv:1012.3138 \[hep-ex\]](#).
158. CDF Collaboration (T. Aaltonen *et al.*), *Phys. Rev. D* **83**, 032008 (2011), [arXiv:1004.4855 \[hep-ex\]](#).
159. CDF Collaboration (T. Aaltonen *et al.*), *Phys. Rev. D* **84**, 052012 (2011), [arXiv:1106.3682 \[hep-ex\]](#).
160. K. Hartkorn and H. Moser, *Eur. Phys. J.* **C8**, 381 (1999).
161. CDF Collaboration (T. Aaltonen *et al.*), *Phys. Rev. Lett.* **107**, 272001 (2011), [arXiv:1103.1864 \[hep-ex\]](#).
162. DØ Collaboration (V. Abazov *et al.*), *Phys. Rev. Lett.* **97**, 241801 (2006), [arXiv:hep-ex/0604046 \[hep-ex\]](#).
163. DØ Collaboration (V. Abazov *et al.*), *Phys. Rev. Lett.* **94**, 042001 (2005), [arXiv:hep-ex/0409043 \[hep-ex\]](#).
164. CDF Collaboration (D. Acosta *et al.*), *Phys. Rev. Lett.* **94**, 101803 (2005), [arXiv:hep-ex/0412057 \[hep-ex\]](#).
165. CDF Collaboration (A. Abulencia *et al.*), *Phys. Rev. Lett.* **97**, 012002 (2006), [arXiv:hep-ex/0603027 \[hep-ex\]](#).
166. DØ Collaboration (V. Abazov *et al.*), *Phys. Rev. Lett.* **102**, 092001 (2009), [arXiv:0805.2614 \[hep-ex\]](#).
167. CDF Collaboration (T. Aaltonen *et al.*), *Phys. Rev. D* **87**, 011101 (2013), [arXiv:1210.2366 \[hep-ex\]](#).
168. S. Stone (2014), [arXiv:1406.6497 \[hep-ex\]](#), and references therein.
169. K. Hagiwara *et al.*, *Phys. Rev. D* **66**, 010001+ (2002), Particle Data Group.
170. DØ Collaboration (V. Abazov *et al.*), *Phys. Rev. Lett.* **99**, 182001 (2007), [arXiv:0706.2358 \[hep-ex\]](#).
171. CDF Collaboration (T. Aaltonen *et al.*), *Phys. Rev. Lett.* **104**, 102002 (2010), [arXiv:0912.3566 \[hep-ex\]](#).
172. CDF Collaboration (A. Abulencia *et al.*), *Phys. Rev. Lett.* **98**, 122001 (2007), [arXiv:hep-ex/0609021 \[hep-ex\]](#).
173. E. Eichten and B. R. Hill, *Phys. Lett. B* **234**, 511 (1990).
174. Y.-b. Dai and M.-q. Huang, *Phys. Rev. D* **59**, 034018 (1999),

- arXiv:hep-ph/9807461 [hep-ph].
175. CDF Collaboration (A. Abulencia *et al.*), *Phys.Rev.Lett.* **96**, 231801 (2006), arXiv:hep-ex/0602005 [hep-ex].
 176. DØ Collaboration (V. Abazov *et al.*), *Phys. Rev. D* **79**, 111102 (2009), arXiv:0805.2576 [hep-ex].
 177. DØ Collaboration (V. M. Abazov *et al.*), *Phys. Rev. D* **85**, 011103 (2012), arXiv:1110.4272 [hep-ex].
 178. CDF Collaboration (T. Aaltonen *et al.*), *Phys. Rev. D* **83**, 052012 (2011), arXiv:1102.1961 [hep-ex].
 179. DØ Collaboration (V. M. Abazov *et al.*), *Phys. Rev. D* **86**, 092011 (2012), arXiv:1204.5723 [hep-ex].
 180. CDF Collaboration (A. Abulencia *et al.*), *Phys. Rev. Lett.* **98**, 061802 (2007), arXiv:hep-ex/0610045 [hep-ex].
 181. DØ Collaboration (V. Abazov *et al.*), *Phys. Rev. Lett.* **99**, 241801 (2007), arXiv:hep-ex/0702049 [hep-ex].
 182. DØ Collaboration (V. Abazov *et al.*), *Phys. Rev. Lett.* **102**, 091801 (2009), arXiv:0811.2173 [hep-ex].
 183. CDF Collaboration (T. Aaltonen *et al.*), *Phys. Rev. Lett.* **100**, 021803 (2008).
 184. CDF Collaboration (T. Aaltonen *et al.*), *Phys. Rev. Lett.* **108**, 201801 (2012), arXiv:1204.0536 [hep-ex].
 185. CDF Collaboration (T. Aaltonen *et al.*), *Phys. Rev. Lett.* **103**, 191802 (2009), arXiv:0809.0080 [hep-ex].
 186. CDF Collaboration (A. Abulencia *et al.*), *Phys. Rev. Lett.* **98**, 122002 (2007), arXiv:hep-ex/0601003 [hep-ex].
 187. CDF Collaboration (T. Aaltonen *et al.*), *Phys. Rev. D* **85**, 032003 (2012), arXiv:1112.3334 [hep-ex].
 188. Belle Collaboration (M. Staric *et al.*), *Phys. Rev. Lett.* **98**, 211803 (2007), arXiv:hep-ex/0703036 [hep-ex].
 189. BaBar Collaboration (J. Lees *et al.*), *Phys. Rev. D* **87**, 012004 (2013), arXiv:1209.3896 [hep-ex].
 190. CDF Collaboration (T. Aaltonen *et al.*), *Phys. Rev. Lett.* **100**, 121802 (2008), arXiv:0712.1567 [hep-ex].
 191. CDF Collaboration (T. A. Aaltonen *et al.*), *Phys. Rev. Lett.* **111**, 231802 (2013), arXiv:1309.4078 [hep-ex].
 192. DØ Collaboration (V. Abazov *et al.*), *Phys. Rev. D* **74**, 112002 (2006), arXiv:hep-ex/0609034 [hep-ex].
 193. DØ Collaboration (V. M. Abazov *et al.*), *Phys. Rev. D* **89**, 012002 (2014), arXiv:1310.0447 [hep-ex].
 194. UA1 Collaboration (C. Albajar *et al.*), *Phys. Lett. B* **186**, 247 (1987).
 195. ARGUS Collaboration (H. Albrecht *et al.*), *Phys. Lett. B* **192**, 245 (1987).
 196. DØ Collaboration (V. Abazov *et al.*), *Phys. Rev. Lett.* **97**, 021802 (2006), arXiv:hep-ex/0603029 [hep-ex].
 197. CDF Collaboration (A. Abulencia *et al.*), *Phys.Rev.Lett.* **97**, 062003 (2006), arXiv:hep-ex/0606027 [hep-ex].
 198. CDF Collaboration (A. Abulencia *et al.*), *Phys. Rev. Lett.* **97**, 242003 (2006), arXiv:hep-ex/0609040 [hep-ex].
 199. CKMfitter Collaboration (J. Charles *et al.*), *Eur. Phys. J.* **C41**, 1 (2005), arXiv:hep-ph/0406184 [hep-ph], updated results and plots available at: <http://ckmfitter.in2p3.fr>.
 200. UTfit Collaboration (M. Bona *et al.*), *JHEP* **0610**, 081 (2006),

- arXiv:hep-ph/0606167 [hep-ph].
201. R. Aleksan, A. Le Yaouanc, L. Oliver, O. Pene and J. Raynal, *Phys. Lett. B* **316**, 567 (1993).
 202. I. Dunietz, R. Fleischer and U. Nierste, *Phys. Rev. D* **63**, 114015 (2001), arXiv:hep-ph/0012219 [hep-ph].
 203. DØ Collaboration (V. M. Abazov *et al.*), *Phys. Rev. D* **85**, 032006 (2012), arXiv:1109.3166 [hep-ex].
 204. DØ Collaboration (V. Abazov *et al.*), *Phys. Rev. Lett.* **101**, 241801 (2008), arXiv:0802.2255 [hep-ex].
 205. DØ Collaboration (V. Abazov *et al.*), *Phys. Rev. D* **76**, 057101 (2007), arXiv:hep-ex/0702030 [hep-ex].
 206. DØ Collaboration (V. Abazov *et al.*), *Phys. Rev. Lett.* **98**, 121801 (2007), arXiv:hep-ex/0701012 [hep-ex].
 207. CDF Collaboration (T. Aaltonen *et al.*), *Phys. Rev. Lett.* **100**, 121803 (2008), arXiv:0712.2348 [hep-ex].
 208. CDF Collaboration (T. Aaltonen *et al.*), *Phys. Rev. Lett.* **100**, 161802 (2008), arXiv:0712.2397 [hep-ex].
 209. CDF Collaboration (T. Aaltonen *et al.*), *Phys. Rev. D* **85**, 072002 (2012), arXiv:1112.1726 [hep-ex].
 210. CDF Collaboration (T. Aaltonen *et al.*), *Phys. Rev. Lett.* **109**, 171802 (2012), arXiv:1208.2967 [hep-ex].
 211. A. Lenz and U. Nierste (2011), arXiv:1102.4274 [hep-ph].
 212. P. Huet and E. Sather, *Phys. Rev. D* **51**, 379 (1995), arXiv:hep-ph/9404302 [hep-ph].
 213. CDF Collaboration (D. Acosta *et al.*), *Phys. Rev. Lett.* **94**, 122001 (2005), arXiv:hep-ex/0504006 [hep-ex].
 214. CDF Collaboration (T. Aaltonen *et al.*), *Phys. Rev. D* **85**, 012009 (2012), arXiv:1111.5023 [hep-ex].
 215. Y. Grossman, A. L. Kagan and Y. Nir, *Phys. Rev. D* **75**, 036008 (2007), arXiv:hep-ph/0609178 [hep-ph].
 216. LHCb Collaboration (R. Aaij *et al.*), *Phys. Rev. Lett.* **108**, 111602 (2012), arXiv:1112.0938 [hep-ex].
 217. CDF Collaboration (T. Aaltonen *et al.*), *Phys. Rev. Lett.* **109**, 111801 (2012), arXiv:1207.2158 [hep-ex].
 218. CDF Collaboration (T. Aaltonen *et al.*), *Phys. Rev. D* **86**, 032007 (2012), arXiv:1207.0825 [hep-ex].
 219. DØ Collaboration (V. M. Abazov *et al.*), *Phys. Rev. Lett.* **112**, 111804 (2014), arXiv:1312.0741 [hep-ex].
 220. DØ Collaboration (V. M. Abazov *et al.*), *Phys. Rev. D* **90**, 111102 (2014), arXiv:1408.6848 [hep-ex].
 221. CDF Collaboration (R. Blair *et al.*) (1996), FERMILAB-DESIGN-1996-01, FERMILAB-PUB-96-390-E.
 222. CDF Collaboration (A. Abulencia *et al.*), *Phys. Rev. Lett.* **97**, 211802 (2006), arXiv:hep-ex/0607021 [hep-ex].
 223. Particle Data Group Collaboration (W. Yao *et al.*), *J. Phys.* **G33**, 1 (2006).
 224. CDF Collaboration (T. Aaltonen *et al.*), *Phys. Rev. Lett.* **103**, 031801 (2009), arXiv:0812.4271 [hep-ex].
 225. Belle Collaboration (S. Lin *et al.*), *Nature* **452**, 332 (2008).
 226. BaBar Collaboration (B. Aubert *et al.*), *Phys. Rev. Lett.* **99**, 021603 (2007), arXiv:hep-ex/0703016 [hep-ex].

227. BaBar Collaboration (B. Aubert *et al.*), *Phys. Rev. D* **76**, 091102 (2007), [arXiv:0707.2798 \[hep-ex\]](#).
228. Y. Keum and A. Sanda, *Phys. Rev. D* **67**, 054009 (2003), [arXiv:hep-ph/0209014 \[hep-ph\]](#).
229. M. Beneke and M. Neubert, *Nucl. Phys.* **B675**, 333 (2003), [arXiv:hep-ph/0308039 \[hep-ph\]](#).
230. CDF Collaboration (T. Aaltonen *et al.*), *Phys. Rev. Lett.* **106**, 181802 (2011), [arXiv:1103.5762 \[hep-ex\]](#).
231. CDF Collaboration (T. Aaltonen *et al.*), *Phys. Rev. Lett.* **108**, 211803 (2012), [arXiv:1111.0485 \[hep-ex\]](#).
232. LHCb Collaboration (R. Aaij *et al.*), *Phys. Rev. Lett.* **110**, 221601 (2013), [arXiv:1304.6173 \[hep-ex\]](#).
233. CDF Collaboration (T. A. Aaltonen *et al.*), *Phys. Rev. Lett.* **113**, 242001 (2014), [arXiv:1403.5586 \[hep-ex\]](#).
234. CDF Collaboration (D. Acosta *et al.*), *Phys. Rev. Lett.* **95**, 031801 (2005), [arXiv:hep-ex/0502044 \[hep-ex\]](#).
235. Belle Collaboration (K. Chen *et al.*), *Phys. Rev. Lett.* **91**, 201801 (2003), [arXiv:hep-ex/0307014 \[hep-ex\]](#).
236. BaBar Collaboration (B. Aubert *et al.*), *Phys. Rev. D* **69**, 011102 (2004), [arXiv:hep-ex/0309025 \[hep-ex\]](#).
237. DØ Collaboration (V. M. Abazov *et al.*), *Phys. Rev. Lett.* **110**, 241801 (2013), [arXiv:1304.1655 \[hep-ex\]](#).
238. DØ Collaboration (V. Abazov *et al.*), *Phys. Rev. Lett.* **100**, 211802 (2008), [arXiv:0802.3299 \[hep-ex\]](#).
239. D. Atwood, I. Dunietz and A. Soni, *Phys. Rev. Lett.* **78**, 3257 (1997), [arXiv:hep-ph/9612433 \[hep-ph\]](#).
240. D. Atwood, I. Dunietz and A. Soni, *Phys. Rev. D* **63**, 036005 (2001), [arXiv:hep-ph/0008090 \[hep-ph\]](#).
241. CDF Collaboration (T. Aaltonen *et al.*), *Phys. Rev. D* **81**, 031105 (2010), [arXiv:0911.0425 \[hep-ex\]](#).
242. CDF Collaboration (T. Aaltonen *et al.*), *Phys. Rev. D* **84**, 091504 (2011), [arXiv:1108.5765 \[hep-ex\]](#).
243. DØ Collaboration (V. M. Abazov *et al.*), *Phys. Rev. D* **86**, 072009 (2012), [arXiv:1208.5813 \[hep-ex\]](#).
244. DØ Collaboration (V. Abazov *et al.*), *Phys. Rev. Lett.* **110**, 011801 (2013), [arXiv:1207.1769 \[hep-ex\]](#).
245. DØ Collaboration (V. Abazov *et al.*), *Phys. Rev. D* **82**, 012003 (2010), [arXiv:0904.3907 \[hep-ex\]](#).
246. LHCb Collaboration (R. Aaij *et al.*), *Phys. Lett. B* **728**, 607 (2014), [arXiv:1308.1048 \[hep-ex\]](#).
247. DØ Collaboration (V. M. Abazov *et al.*), *Phys. Rev. D* **84**, 052007 (2011), [arXiv:1106.6308 \[hep-ex\]](#).
248. DØ Collaboration (V. M. Abazov *et al.*), *Phys. Rev. Lett.* **105**, 081801 (2010), [arXiv:1007.0395 \[hep-ex\]](#).
249. DØ Collaboration (V. M. Abazov *et al.*), *Phys. Rev. D* **82**, 032001 (2010), [arXiv:1005.2757 \[hep-ex\]](#).
250. DØ Collaboration (V. Abazov *et al.*), *Phys. Rev. D* **74**, 092001 (2006), [arXiv:hep-ex/0609014 \[hep-ex\]](#).
251. G. Borissov and B. Hoeneisen, *Phys. Rev. D* **87**, 074020 (2013), [arXiv:1303.0175 \[hep-ex\]](#).

252. HFAG Collaboration (Y. Amhis *et al.*) (2012), [arXiv:1207.1158 \[hep-ex\]](#), PDG 2011 update, online at http://www.slac.stanford.edu/xorg/hfag/osc/PDG_2011/#BETAS by the Heavy Flavor Averaging Group.
253. CDF Collaboration (T. Aaltonen *et al.*), *Phys. Rev. Lett.* **107**, 261802 (2011), [arXiv:1107.4999 \[hep-ex\]](#).
254. CDF Collaboration (T. Aaltonen *et al.*), *Phys. Rev. D* **82**, 091105 (2010), [arXiv:1008.5077 \[hep-ex\]](#).
255. DØ Collaboration (V. Abazov *et al.*), *Phys. Rev. Lett.* **100**, 101801 (2008), [arXiv:0708.2094 \[hep-ex\]](#).
256. A. J. Buras, J. Girrbach, D. Guadagnoli and G. Isidori, *Eur. Phys. J. C* **72**, 2172 (2012), [arXiv:1208.0934 \[hep-ph\]](#).
257. L3 Collaboration (M. Acciarri *et al.*), *Phys. Lett. B* **391**, 474 (1997).
258. W. Altmannshofer and D. M. Straub, *JHEP* **1208**, 121 (2012), [arXiv:1206.0273 \[hep-ph\]](#).
259. CDF Collaboration (D. Acosta *et al.*), *Phys. Rev. Lett.* **93**, 032001 (2004), [arXiv:hep-ex/0403032 \[hep-ex\]](#).
260. DØ Collaboration (V. Abazov *et al.*), *Phys. Rev. Lett.* **94**, 071802 (2005), [arXiv:hep-ex/0410039 \[hep-ex\]](#).
261. DØ Collaboration (V. Abazov *et al.*), *Phys. Rev. D* **76**, 092001 (2007), [arXiv:0707.3997 \[hep-ex\]](#).
262. DØ Collaboration (V. M. Abazov *et al.*), *Phys. Lett. B* **693**, 539 (2010), [arXiv:1006.3469 \[hep-ex\]](#).
263. DØ Collaboration (V. M. Abazov *et al.*), *Phys. Rev. D* **87**, 072006 (2013), [arXiv:1301.4507 \[hep-ex\]](#).
264. CDF Collaboration (A. Abulencia *et al.*), *Phys. Rev. Lett.* **95**, 221805 (2005), [arXiv:hep-ex/0508036 \[hep-ex\]](#).
265. CDF Collaboration (T. Aaltonen *et al.*), *Phys. Rev. Lett.* **100**, 101802 (2008), [arXiv:0712.1708 \[hep-ex\]](#).
266. CDF Collaboration (T. Aaltonen *et al.*), *Phys. Rev. Lett.* **107**, 191801 (2011), [arXiv:1107.2304 \[hep-ex\]](#).
267. CDF Collaboration (T. Aaltonen *et al.*), *Phys. Rev. D* **87**, 072003 (2013), [arXiv:1301.7048 \[hep-ex\]](#).
268. DØ Collaboration (V. Abazov *et al.*), *Phys. Rev. D* **74**, 031107 (2006), [arXiv:hep-ex/0604015 \[hep-ex\]](#).
269. CDF Collaboration (T. Aaltonen *et al.*), *Phys. Rev. D* **79**, 011104 (2009), [arXiv:0804.3908 \[hep-ex\]](#).
270. CDF Collaboration (T. Aaltonen *et al.*), *Phys. Rev. Lett.* **106**, 161801 (2011), [arXiv:1101.1028 \[hep-ex\]](#).
271. BaBar Collaboration (B. Aubert *et al.*), *Phys. Rev. D* **79**, 031102 (2009), [arXiv:0804.4412 \[hep-ex\]](#).
272. Belle Collaboration (J.-T. Wei *et al.*), *Phys. Rev. Lett.* **103**, 171801 (2009), [arXiv:0904.0770 \[hep-ex\]](#).
273. CDF Collaboration (T. Aaltonen *et al.*), *Phys. Rev. Lett.* **107**, 201802 (2011), [arXiv:1107.3753 \[hep-ex\]](#).
274. CDF Collaboration (T. Aaltonen *et al.*), *Phys. Rev. Lett.* **108**, 081807 (2012), [arXiv:1108.0695 \[hep-ex\]](#).
275. J. C. Pati and A. Salam, *Phys. Rev. D* **10**, 275 (1974).
276. CDF Collaboration (T. Aaltonen *et al.*), *Phys. Rev. Lett.* **102**, 201801 (2009), [arXiv:0901.3803 \[hep-ex\]](#).